© 2018. Published by The Company of Biologists Ltd | Journal of Cell Science (2018) 131, jcs216382. doi:10.1242/jcs.216382

RESEARCH ARTICLE

Adaptive adhesion systems mediate glioma cell invasion in complex environments

Pavlo G. Gritsenko[1] and Peter Friedl[1,2,3,*]

ABSTRACT

Diffuse brain invasion by glioma cells prevents effective surgical or molecular-targeted therapy and underlies a detrimental outcome. Migrating glioma cells are guided by complex anatomical brain structures but the exact mechanisms remain poorly defined. To identify adhesion receptor systems and matrix structures supporting glioma cell invasion into brain-like environments we used 2D and 3D organotypic invasion assays in combination with antibody-, peptide- and RNA-based interference. Combined interference with β1 and αV integrins abolished the migration of U-251 and E-98 glioma cells on reconstituted basement membrane; however, invasion into primary brain slices or 3D astrocyte-based scaffolds and migration on astrocyte-deposited matrix was only partly inhibited. Any residual invasion was supported by vascular structures, as well as laminin 511, a central constituent of basement membrane of brain blood vessels. Multi-targeted interference against β1, αV and α6 integrins expressed by U-251 and E-98 cells proved insufficient to achieve complete migration arrest. These data suggest that mechanocoupling by integrins is relatively resistant to antibody- or peptide-based targeting, and cooperates with additional, as yet unidentified adhesion systems in mediating glioma cell invasion in complex brain stroma.

KEY WORDS: Glioma invasion, Integrins, Laminin, Adhesion plasticity, 3D brain models

INTRODUCTION

Gliomas originate from transformed progenitor cells, in which abnormal brain development programs are combined with unrestricted local growth and diffuse infiltration into the brain stroma (Wen and Reardon, 2016). Glioma cell invasion occurs along defined tissue structures, including white matter tracks comprising myelinated axons and astrocyte processes, forming topologically complex cellular networks filled with hydrated, soft extracellular matrix (ECM) composed of hyaluronan and proteoglycans (Cuddapah et al., 2014; Gritsenko et al., 2012; Miyata and Kitagawa, 2017). As an alternative invasion route, brain blood vessels provide a particularly permissive niche of confined space between vascular basement membranes and adjacent brain stroma, which are molecularly and physically complex types of confined space (Di Russo et al., 2017; Farin et al., 2006; Gritsenko et al., 2012; Watkins et al., 2014). To interact with structural basement membrane proteins, glioma cells depend upon integrin adhesion receptors, including: α3β1, α6β1, α6β4 and α7β1 binding to laminins, α1β1 and α2β1 interacting with type-IV collagen (Kawataki et al., 2007; Khoshnoodi et al., 2008; Ramovs et al., 2017; Yurchenco, 2011, 2015), and αVβ3 engaging with both laminin and type IV collagen (Pedchenko et al., 2004; Sasaki and Timpl, 2001; Xu et al., 2001). Invading glioma cells upregulate several integrin subsets, including α3β1 and αVβ3 integrins (Bello et al., 2001; Paulus et al., 1993; Schittenhelm et al., 2013). For their migration along 2D surfaces or through transwell filters coated with different laminin isoforms and collagen IV or reconstituted basement membrane (rBM; Matrigel), glioma cells depend upon α3β1, α6β1 and α1β1 integrins (Delamarre et al., 2009; Hamaia et al., 2012; Kawataki et al., 2007; Nakada et al., 2013; Wondimu et al., 2013). Whereas the adhesion mechanisms mediating glioma cell migration along rBM are largely established, the adhesion systems supporting perivascular and interstitial invasion in brain tissue remain unclear.

In addition to rBM, other diverse 2D and 3D *in vitro* assays have been developed to model glioma cell invasion into brain stroma (Rao et al., 2014; Rape et al., 2014). 3D collagen scaffolds, broadly used in cancer research, are effectively invaded by glioma cells (Frolov et al., 2016; Kaufman et al., 2005); furthermore, combined targeting of β1 integrin and JNK kinase significantly inhibited glioma cell invasion in type I collagen gels (Vehlow et al., 2017). However, the relevance of fibrillar collagen for the largely collagen-free brain parenchyma remains unclear (Gritsenko et al., 2012; Rape et al., 2014). Cross-linked hyaluronan also supports glioma cell migration (Ananthanarayanan et al., 2011; Gordon et al., 2003), but hyaluronan-based substrates lack cellular components and structural ligands for guidance (Cuddapah et al., 2014; Gritsenko et al., 2012). Astrocytes cultured as 2D monolayers release migration-enhancing molecules and enable gap junctional communication to glioma cells (Hong et al., 2015; Oliveira et al., 2005; Rath et al., 2013), and 3D astrocyte cultures provide additional topologic complexity supporting glioma cell invasion as single cells and multicellular networks (Gritsenko et al., 2017). Rat brain aggregates formed by cells originating from fetal brain reproduce the 3D structure of neuropil without blood vessels (Bjerkvig, 1986). Single-targeted interference of β1 or αVβ3 integrins was largely ineffective in inhibiting glioma invasion into rat brain aggregates, and combinations of targeting other integrin subsets and ligand conditions were not explored (Tonn et al., 1998). As the most complex multi-ligand system currently utilized, brain slice culture provides *in vivo*-like substrate topologies to reproduce glioma cell invasion including radial migration along blood vessels (de Bouard et al., 2002; Fayzullin et al., 2016); however, the adhesion mechanisms mediating glioma cell invasion into brain slices remain unexplored.

To experimentally test the mechanistic variability and adaptability of glioma cell invasion in different brain environments, we apply recently developed complementary

[1]Department of Cell Biology, Radboud Institute for Molecular Life Sciences, Radboud University Nijmegen Medical Centre, 6525 GA Nijmegen, The Netherlands. [2]David H. Koch Center for Applied Research of Genitourinary Cancers, Department of Genitourinary Medical Oncology, The University of Texas, MD Anderson Cancer Center, Houston, 77030 Texas, USA. [3]Cancer Genomics Centre (CGC.nl), 3584 Utrecht, The Netherlands.

*Author for correspondence (Peter.Friedl@radboudumc.nl)

P.F., 0000-0002-0119-4041

Received 31 January 2018; Accepted 2 July 2018

Journal of Cell Science (2018) 131, jcs216382. doi:10.1242/jcs.216382

in vitro models (Gritsenko et al., 2017) and address the role of integrins in mediating adhesive migration along or through rBM and organotypic brain-like 3D environments. Using stringent, multi-inhibitor integrin targeting strategies, we reveal substantial residual glioma invasion competence after interference with integrins in complex brain environments and on a laminin-511-coated surface, suggesting cooperation of integrin-dependent and/or other adhesion systems.

RESULTS

U-251 and E-98 glioma cell lines abundantly expressed α3 and β1 integrin subunits, moderate levels of α6, αV, β3, β4 and negligible levels of α1, α2 integrins (Fig. S1). Based on known subunit combinations, both cell lines thus expressed predominantly α3β1 and α6β1 integrin heterodimers, indicating a combined ligand preference for laminins (Nishiuchi et al., 2003, 2006). Compared with E-98 cells, U-251 expressed higher levels of αVβ3, an RGD-dependent integrin with broad substrate specificity (Demircioglu and Hodivala-Dilke, 2016; Goodman and Picard, 2012).

In reference to published work (Benton et al., 2014), we tested the role of integrins in the emigration of U-251 and E-98 cells from spheroids on rBM. Combined antibody and peptide targeting of β1 and αV integrins, but not individual interference, abrogated migration of U-251 cells in this assay, confirming both integrin subsets as essential for U-251 cell migration on rBM (Fig. S2A,B). Compared with U-251 cells, E-98 cells migrating on rBM were more sensitive to targeting of β1 integrin (Fig. S2A,B), indicating a more-restricted substrate preference, possibly due to limited αVβ3 integrin availability (Fig. S1). The relevance of β1 and αV integrins in supporting migration of both cell types was confirmed using a 3D

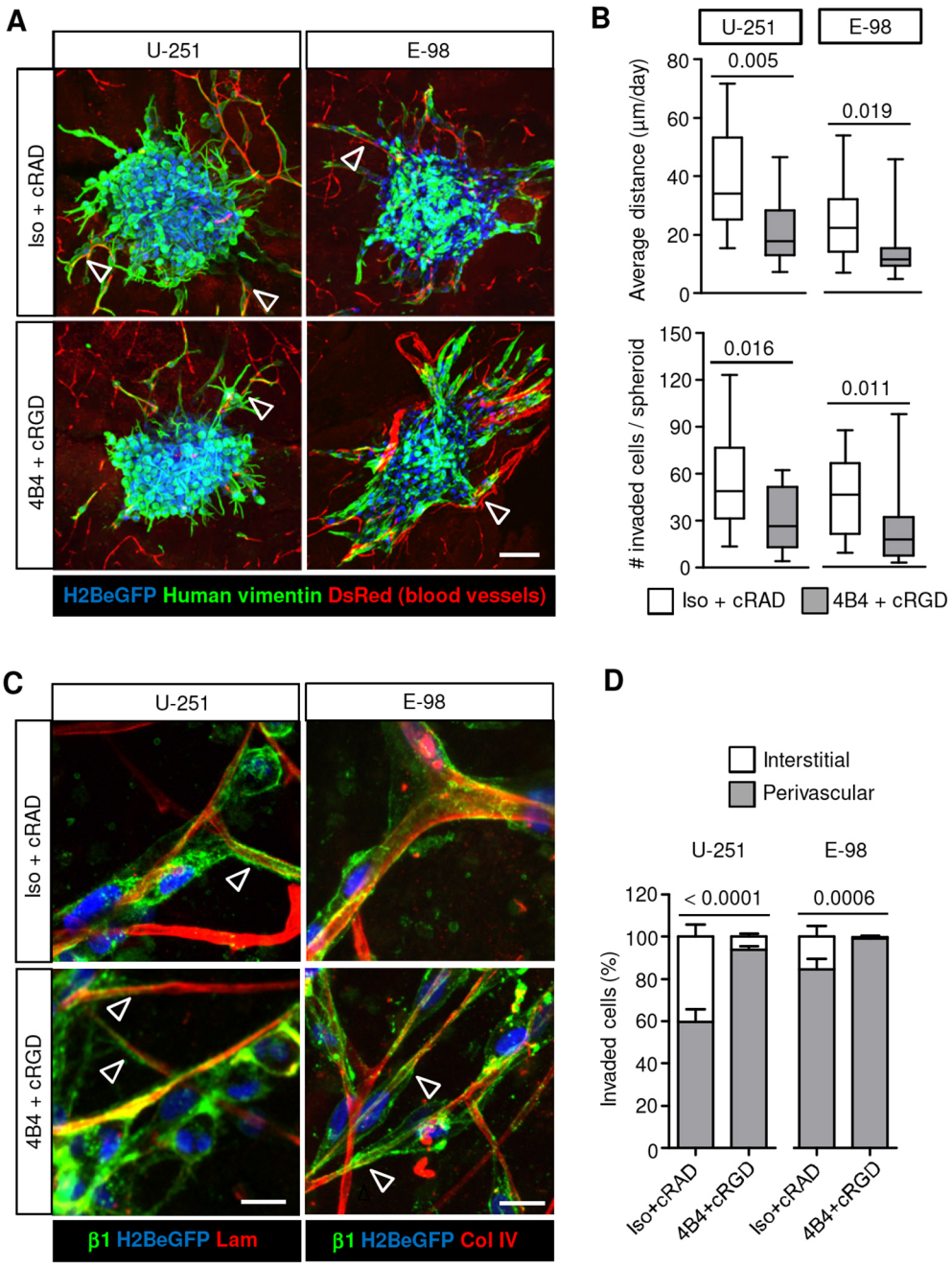

Fig. 1. Targeting β1 and αV integrin induces partial inhibition of glioma cell invasion along blood vessels in mouse brain slices. (A) Invasion of U-251 and E-98 cells from spheroids after culture for 2 days in the presence of isotypic IgG1 and cRADfV control peptide or adhesion-perturbing human-specific anti-β1-integrin 4B4 antibody and cRGDfV peptide. Red signal originates from ubiquitously expressed DsRed contrasting vessels (bright signals) and stromal cells (dim signal). Arrowheads indicate glioma cells that have invaded along blood vessels. (B) Average invasion distance of glioma cells from the spheroid margin and the number of invaded cells per spheroid. Data represent 16 and 15 (U-251), 20 and 17 (E-98) spheroids per control and integrin interference condition, respectively from three independent experiments. Values display the median (black line), 25th and 75th percentiles (boxes), and maximum and minimum (whiskers). *P*-values shown were obtained using the Mann-Whitney test. (C) Invasion along capillaries in the presence of 4B4 mAb and cRGDfV peptide. Anti-β1-integrin mAb 4B4 is visualized with Alexa Fluor-conjugated secondary antibody after fixation (green). Basement membranes are stained with anti-laminin or -collagen IV. Arrowheads indicate elongated glioma cells and protrusions interacting with basement membrane of capillaries. (D) Vessel-associated or interstitial position of glioma cells invading brain slices in the presence or absence of integrin targeting from three independent experiments. Percentage of glioma cells invading from multicellular spheroids into the brain slices associated or not associated with vessels is shown. Data represent the same number of spheroids indicated in B. Values display the mean ±s.e.m. from three independent experiments. *P*-values shown were obtained using the Mann-Whitney test (for perivascular position). Scale bars: 100 µm (A), 20 µm (C).

Journal of Cell Science (2018) 131, jcs216382. doi:10.1242/jcs.216382

rBM-hyaluronan interface assay (Fig. S2C,D), suggesting that rBM but not hyaluronan is the dominant invasion-promoting substrate.

When cultured on 3D organotypic brain slices, U-251 and E-98 cells invaded preferentially along blood vessels (Fig. 1A,D), and combined anti-β1 or -αV integrin interference decreased the distance migrated and the total number of cells that had invaded by ∼50-60% (Fig. 1B). Despite the abundant level of an adhesion-perturbing antibody (4B4) at the cell surface, detected by post-fixation confocal microscopy using secondary antibody only (Fig. 1C, green channel), glioma cell elongation and their interaction with capillary basement membranes remained intact during emigration from spheroids (Fig. 1C, arrowheads). Notably, the fraction of migrating glioma cells associated with blood vessels increased significantly in response to integrin inhibition (Fig. 1D). This compartmental transition after interference with integrins indicates differential adhesion requirements in the invasion of perivascular space versus interstitial tissue.

To address the mechanisms of interstitial glioma cell invasion directly, astrocyte-generated 3D scaffolds containing both living astrocytes and ECM deposited by astrocytes were used as a migration substrate (Gritsenko et al., 2017). Emigrating from spheroids, U-251 and E-98 cells infiltrated astrocyte scaffolds by moving between astrocyte boundaries (Fig. 2A). Similarly to invasion of brain slices, infiltration into astrocyte scaffolds was reduced by ∼50-60% by dual-targeting of β1 and αV integrins, whereas the total number of invaded cells was decreased more profoundly, up to ∼70-90% (Fig. 2B). The differential sensitivity to interference suggests that cell detachment from the spheroid and the migration thereafter depend on distinct adhesion thresholds mediated by integrins. To discern whether the cell or matrix components primarily support glioma cell invasion in this assay, astrocyte-deposited matrix was decellularized and used as a migration substrate. Whereas inhibition of migration on rBM was complete after interference with β1 and αV integrin subunits, the inhibition of glioma cell migration on astrocyte-deposited matrix was less efficient, with reductions of up to 95% (U-251) or 60% (E-98) (Fig. 3A-C). Similar residual migration in E-98 cells was obtained on matrix deposited by human astrocytes and no further inhibition was achieved by addition of anti-αV or -α6 antibody (Fig. 3C-E). Thus, in contrast to glioma cell migration along rBM, which could be abrogated by antibody- and peptide-based interference of integrins (Fig. 3B,C,E), invasion into brain slices, 3D astrocyte scaffolds or along astrocyte-deposited matrix were less affected by these inhibition schemes.

To identify the underlying protein repertoire, astrocyte-deposited matrices were analysed by mass spectrometry. Nine and 22 ECM proteins were identified in murine and human astrocyte matrices, respectively (Fig. S3A-C; Tables S2 and S3). Besides laminin 111, type-IV collagen, nidogen, perlecan and fibronectin, which were present in both astrocyte-deposited ECM and rBM, laminin α5 was detected in astrocyte cultures but largely absent in rBM (Hughes et al., 2010). Laminin α5 contributes to laminin 511, the predominant isoform in basement membranes of brain blood vessels (Di Russo et al., 2017; Wu et al., 2009). To test whether laminin 511 accounts for integrin-dependent or integrin-independent glioma-cell–matrix interactions, cell culture plastic coated with human recombinant laminin 511 was used as a migration substrate. Combined β1 and αV integrin interference decreased U-251 cell migration on laminin 511 by 28%, whereas the migration of E-98 cells was not significantly changed (Fig. 4A,B). However, this treatment did ablate U-251 and E-98 migration on laminin 211, type IV collagen, fibronectin and rBM (Fig. 4B and Fig. S4A,B), confirming the technical stringency of the dual-interference strategy and revealing the pro-migratory properties of laminin 511 beyond β1 and αV integrin engagement.

Principal cell receptors for adhesion to laminin 511 include α3β1, α6β1, α6β4 and α7β1 integrins (Nishiuchi et al., 2003; Nishiuchi

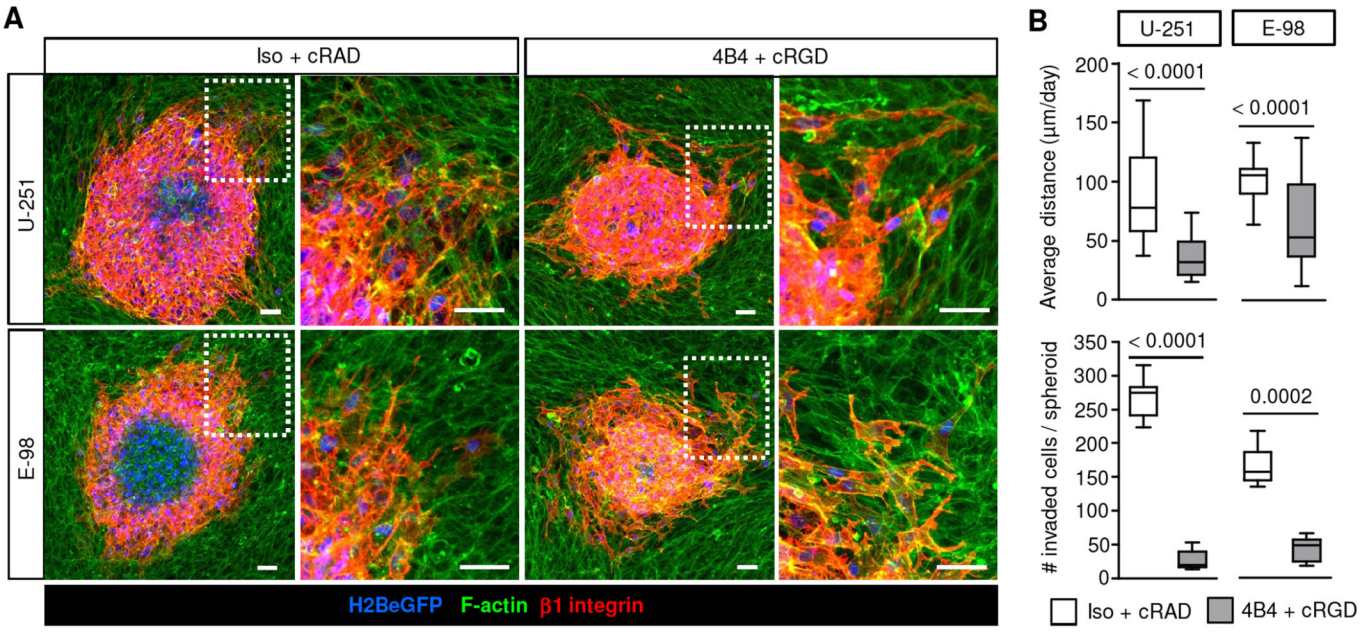

Fig. 2. Targeting β1 and αV integrin induces partial inhibition of glioma cell invasion in 3D mouse astrocyte scaffolds. (A) Invasion of U-251 and E-98 cells from spheroids after culture for 2 days in 3D astrocyte scaffolds in the presence of isotypic IgG1 (Iso) and cRADfV control peptide or adhesion-perturbing anti-β1-integrin antibody (4B4) and cRGDfV peptide. (B) Average invasion distance of U-251 and E-98 cells from the spheroid margin and the total number of invaded cells. Data represent 41 and 37 (U-251), or 36 and 43 (E-98) spheroids per control and integrin interference condition, respectively from three independent experiments. Values display the median (black line), 25th and 75th percentiles (boxes), and maximum and minimum (whiskers) from three independent experiments. *P*-values shown were obtained using the Mann–Whitney test. Scale bars: 50 µm.

Journal of Cell Science (2018) 131, jcs216382. doi:10.1242/jcs.216382

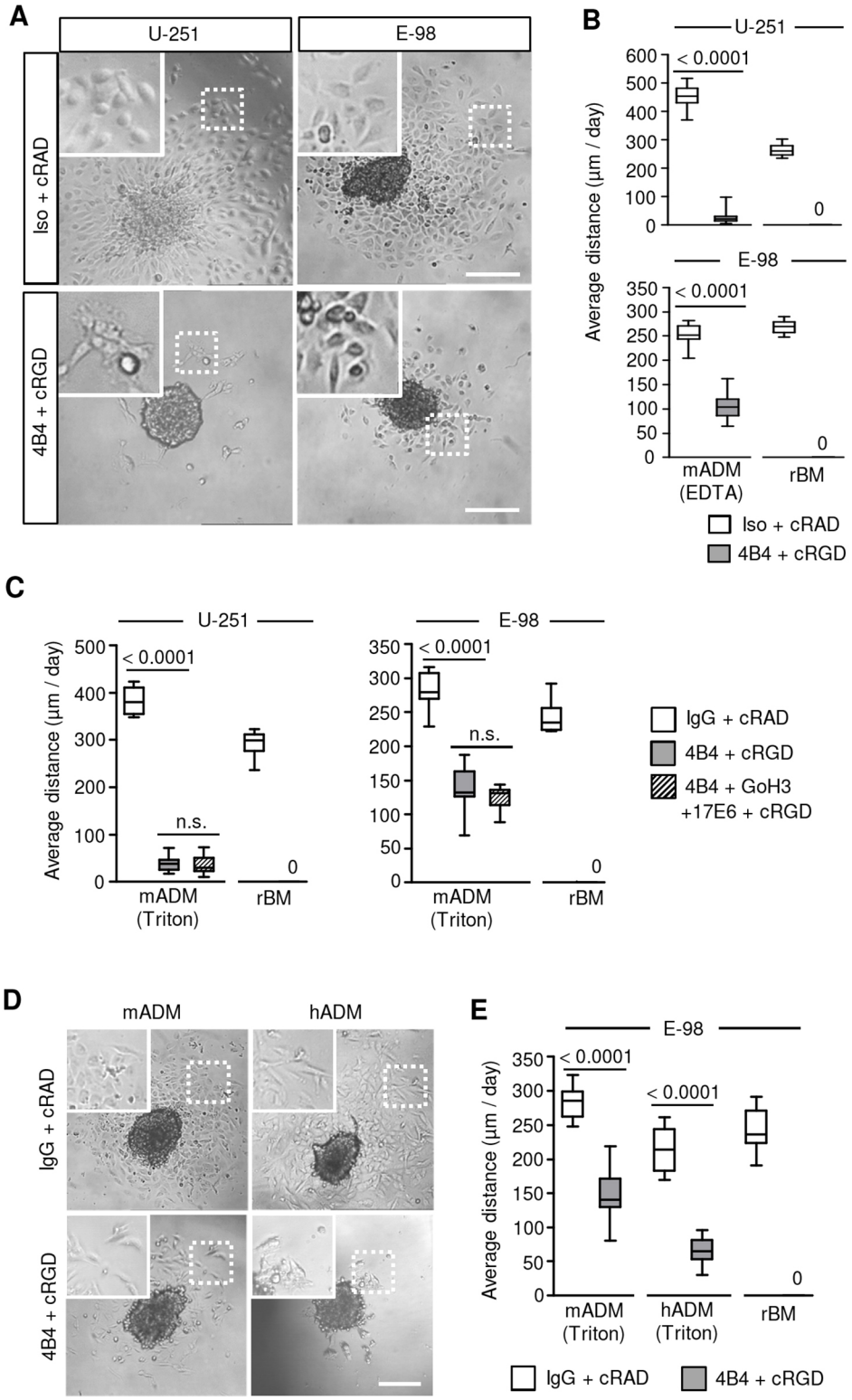

Fig. 3. Interference with β1 and αV integrins abolishes migration of glioma cells on rBM but not astrocyte-deposited matrix. (A) Overviews and (B) average migration distance of U-251 and E-98 cells from spheroids after 24 hours on mouse astrocyte-deposited matrix (mADM) or rBM in the presence of isotypic IgG and cRADfV control peptide or the adhesion-perturbing antibodies 4B4 (β1), 17E6 (αV) and GoH3 (α6), and cRGDfV peptide. Mouse astrocytes were cultured for 3 days and (B) removed from culture surface with 0.002 M EDTA only, or (C) the culture surface was additionally treated with 0.25% Triton X-100 and 0.25% sodium deoxycholate in PBS. (D) Overviews and (E) average migration distance of E-98 cells from spheroids on mouse (mADM) or human (hADM) astrocyte-deposited matrix. Mouse and human astrocytes were cultured for 3 or 7 days, respectively, and removed with 0.002 M EDTA followed by treatment of culture surface with 0.25% Triton X-100 and 0.25% sodium deoxycholate in PBS. Data represent on average 10-22 spheroids per condition from three independent experiments. Values display the median (black line), 25th and 75th percentiles (boxes), and maximum and minimum (whiskers). *P*-values shown were obtained using the Mann-Whitney test. n.s., not significant. Scale bars: 200 µm.

et al., 2006). To address whether glioma cells moving on laminin 511 after dual-integrin targeting still develop focal adhesions, samples were stained for paxillin, a structural protein contributing to integrin–actin-filament linkage (Schaller, 2001). U-251 and E-98 cells, in the absence or presence of β1 or αV integrin inhibitors, formed string-like focalized enrichments consistent with focal adhesions (Fig. 4C), suggesting residual integrin-mediated adhesion or an alternative laminin 511-binding mechanism. To address whether inhibition of β1 integrin by monoclonal antibodies was incomplete, siRNA-mediated transient downregulation of β1 integrin was combined with antibody- and peptide-based β1 and αV integrin interference. β1 integrin siRNAs caused a 73-88% reduction of cell surface levels of β1 subunits in the majority of cells detected by flow cytometry (Fig. S5A) or confocal microscopy (Fig. S5B). When compared with dual-

Journal of Cell Science (2018) 131, jcs216382. doi:10.1242/jcs.216382

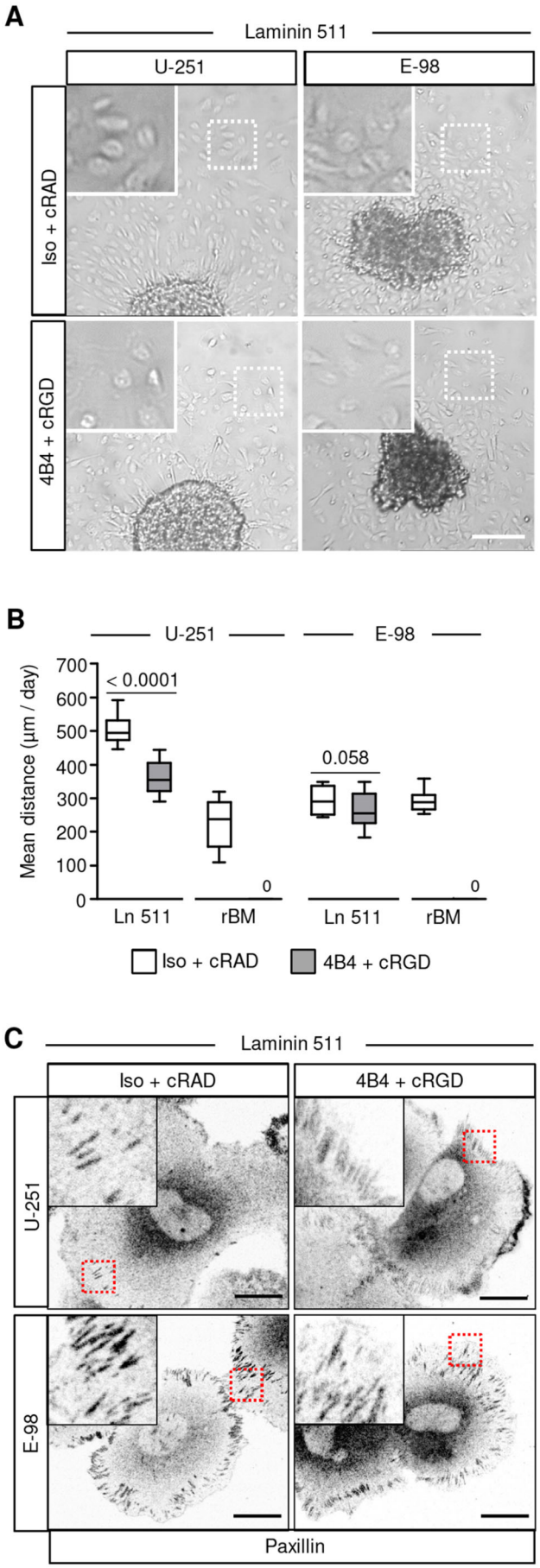

Fig. 4. Glioma cells effectively migrate and form focal adhesions on laminin 511 in the presence of β1 and αV integrin inhibitors. (A) Migration of U-251 and E-98 cells from spheroids after 24 h on a plastic surface coated with laminin 511 in medium with isotypic IgG1 and control cRADfV peptide or with adhesion-perturbing anti β1 integrin 4B4 mAb and cRGDfV peptide. (B) Migration distance of U-251 and E-98 cells on plastic surfaces coated with laminin 511. Data represent 16-17 (U-251) or 17 (E-98) spheroids per condition on laminin 511, and 16 (U-251) or 13-18 (E-98) spheroids per condition on rBM from three independent experiments. Values display the median (black line), 25th and 75th percentiles (boxes), and maximum and minimum (whiskers). *P*-values shown were obtained using the Mann-Whitney test. (C) Paxillin staining in E-98 and U-251 cells that radially migrated from spheroids on astrocyte-deposited matrix or laminin-511-coated surface. Scale bars: 200 µm (A) and 25 µm (C).

targeting of integrins, this triple interference further enhanced the inhibition efficiency by up to 40% (U-251) and 60% (E-98) on laminin 511 (Fig. 5A,B and Fig. S5C), and by ∼30% in 3D astrocyte scaffolds (Fig. 5A,B). To further test whether α6β4 integrin (expressed by U-251 but not E-98 cells; Fig. S1) supports migration, adhesion-perturbing anti-α6 integrin monoclonal antibody (Sonnenberg et al., 1987) was combined with our triple-interference strategy described above (Fig. 6A-C). This quadruple interference strategy did not yield any additional inhibition of U-251 cell invasion in 3D astrocyte scaffolds or migration on a laminin-511-coated surface (Fig. 6D). Despite the additive effects reached by combinatorial integrin targeting, residual migration distances of ∼20 or 200 µm/day in astrocyte scaffolds and on laminin 511, respectively, was remarkably retained.

DISCUSSION

Our data suggest that β1 and αV integrins represent the primary adhesion systems for glioma cell migration in different migration models. However, when comparing the same interference strategy, the contribution of integrin-dependent glioma invasion varies and glioma cells consistently demonstrated residual migration in complex brain-like environments or on purified laminin-511-coated surfaces, suggesting that alternative interaction strategies are complex brain-like models.

Major constituents of brain basement membranes include type IV collagen and the laminin isoforms 511, 211, 332, 111 (Di Russo et al., 2017; Kawataki et al., 2007; Yurchenco, 2015). rBM, a popular substrate that reproduces aspects of basement membranes *in vitro* based on its content of laminin 111 and type IV collagen (Hughes et al., 2010), lacks important brain-related laminin isoforms and differs from the ligand heterogeneity of ECM deposited by astrocytes, endothelium pericytes and glioma cells (Di Russo et al., 2017; Kawataki et al., 2007). The particularly high sensitivity of glioma cell migration on rBM to β1 and αV integrin dual-interference thus overestimates the relevance of integrin-mediated migration, whereas basement membranes in the brain slices and 3D astrocyte scaffolds likely support both integrin-dependent and integrin-independent, alternative mechanisms of migration.

By mass-spectrometry analysis of the astrocyte-deposited matrices, we identified laminin 511 as a basement membrane constituent, which supports glioma cell migration and focalized adhesion formation. Laminin 511 is a multifunctional adhesion protein ubiquitously expressed in the basement membranes of different tissue structures including brain blood vessels (Pouliot and Kusuma, 2013; Spenlé et al., 2013; Yousif et al., 2013). Integrins α3β1, α6β1, α6β4 and α7β1 are the major receptors mediating cell adhesion on laminin 511 (Nishiuchi et al., 2003, 2006) and αVβ3 integrin can provide additional interactions to this laminin isoform

Journal of Cell Science (2018) 131, jcs216382. doi:10.1242/jcs.216382

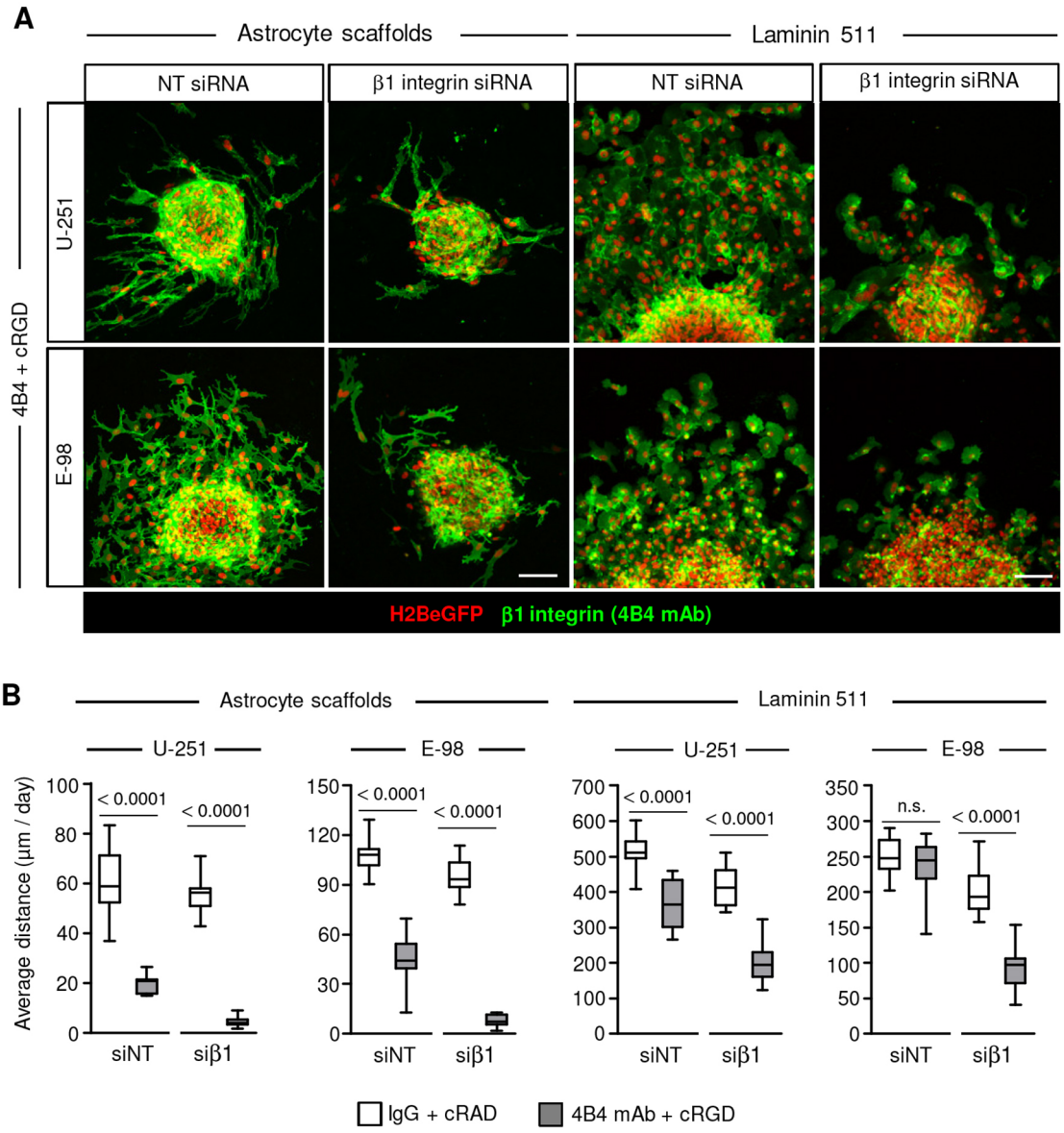

Fig. 5. β1 integrin subunits mediate glioma cell migration on laminin 511 and invasion in 3D astrocyte scaffolds. (A) Migration of U-251 and E-98 cells, transfected with non-targeting control (NT) siRNAs or anti-β1-integrin siRNAs, from spheroids on laminin-511-coated culture surface (24 h) and the cell invasion in 3D astrocyte scaffolds (48 h), in medium with isotypic IgG1 and control cRADfV peptide or adhesion-perturbing anti-β1-integrin 4B4 mAb combined with cRGDfV peptide. (B) Average migration distance of U-251 and E-98 cells on plastic surface coated with laminin 511 and invasion in 3D astrocyte scaffolds. Data represent 15-16 (U-251) or 15-18 (E-98) spheroids per condition in astrocyte scaffolds, and 16-32 (U-251) or 15-24 (E-98) spheroids per condition on laminin 511 from three independent siRNA transfections. Values display the median (black line), 25th and 75th percentiles (boxes), and maximum and minimum (whiskers). *P*-values shown were obtained using the Mann-Whitney test. n.s., not significant. Scale bars: 100 µm.

(Sasaki and Timpl, 2001). Laminin 511 contains independent binding sites for α3β1 and αVβ3 integrins (Ido et al., 2004; Kikkawa et al., 2007; Nielsen and Yamada, 2001; Sasaki and Timpl, 2001) and may engage multiple integrin subtypes simultaneously in a non-competitive manner. Accordingly, β1 integrin is the predominant subunit expressed by U-251 and E-98 cells and other glioma models (Kawataki et al., 2007), and mediates migration along laminin 511 in both cell types; however, significant residual migration was retained despite dual- and multi-targeted interference. Incomplete inhibition resulting from overlapping mechanisms may be one possible explanation. β1 integrins interact with laminin 511 with high affinity (Nishiuchi et al., 2003, 2006) and thus may outcompete the antagonistic efficacy of the integrin inhibitors. In addition, laminin 511 contains binding sites for non-integrin cell surface receptors, including Lu/B-CAM, α-dystroglycan and syndecan-4 (Kikkawa et al., 2007, 2013; Lin and Kurpakus-Wheater, 2002; Shimizu et al., 1999), which may substitute for integrin-mediated force generation.

In addition to receptor-dependent interaction with laminin, glioma cell invasion along confined spaces between the stroma–blood-vessel interface or dense astrocyte scaffolds may occur through non-adhesive, physical mechanisms, mediated by tubulin polymerization, myosin II contraction and/or ion channel-mediated alterations of cytoplasmic volume (Balzer et al., 2012; Beadle et al., 2008; Katsetos et al., 2015; Panopoulos et al., 2011; Paul et al., 2017; Thompson and Sontheimer, 2016). The relative contribution of adhesive versus non-adhesive mechanisms of glioma invasion in organotypic assays *in vitro* and their relevance to the invasion

Journal of Cell Science (2018) 131, jcs216382. doi:10.1242/jcs.216382

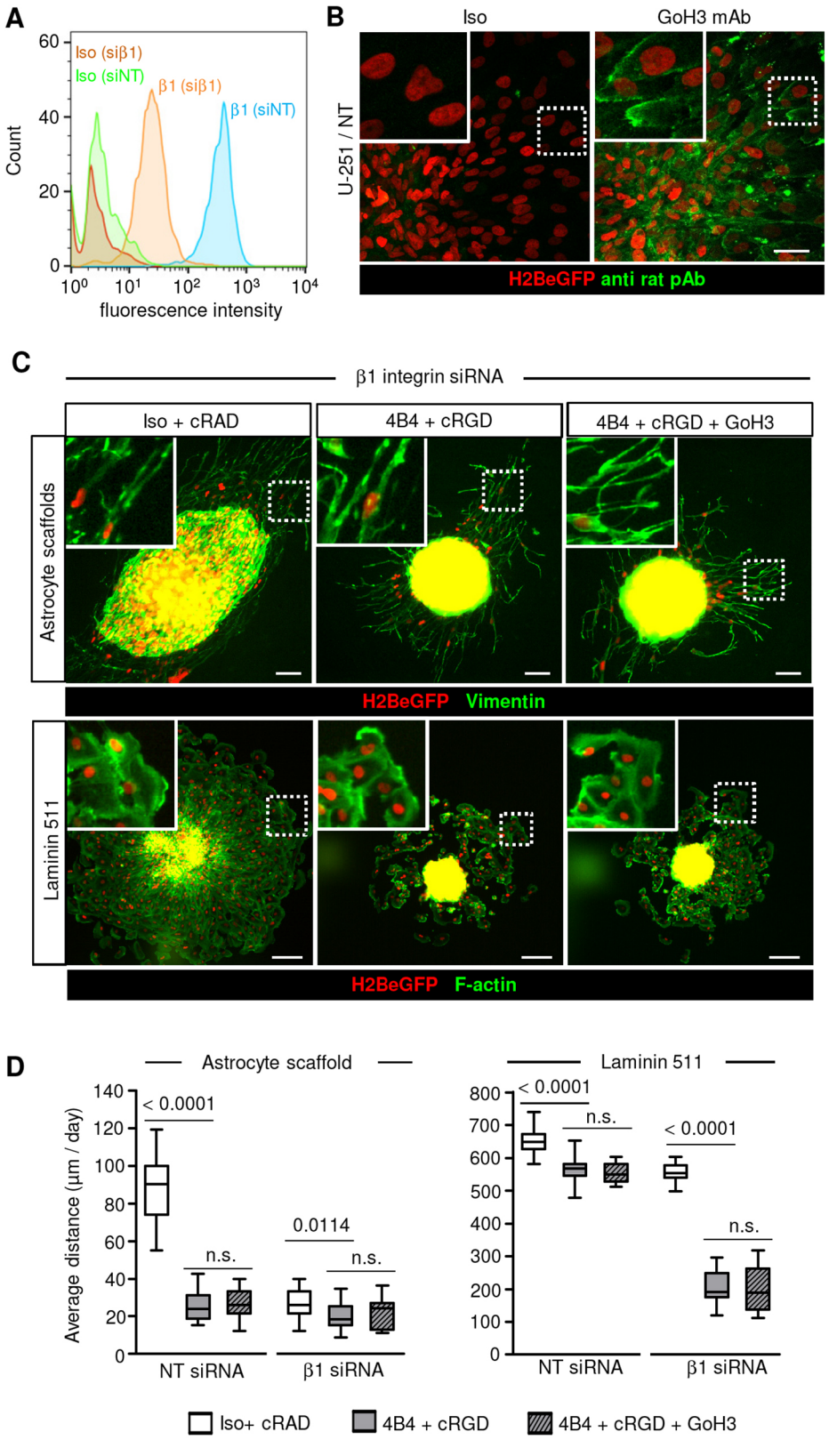

Fig. 6. Residual migration of U-251 cells after β1, αV and α6 integrin interference.
(A) Surface levels of β1 integrin in U-251 cells 3 days after transfection with either NT or β1 integrin siRNA detected by flow cytometry. (B) Binding of anti-α6-integrin antibody GoH3 but not isotypic IgG2 by migrating U-251 cells in spheroid culture on laminin 511. (C) Migration of U-251 cells from spheroids on laminin 511 (24 h) or in 3D mouse astrocyte scaffold culture (48 h) after multi-targeted interference, as indicated. Glioma cells invading astrocyte scaffolds were identified by human-specific vimentin staining (green) and nuclear H2BeGFP. (D) Average migration distance of U-251 cells on laminin 511 or into 3D astrocyte scaffolds. Data represent 19-33 spheroids per condition in astrocyte scaffolds and 17-20 spheroids per condition on laminin 511 from three independent siRNA transfections. Values display the median (black line), 25th and 75th percentiles (boxes), and maximum and minimum (whiskers). *P*-values shown were obtained using the Mann-Whitney test. n.s., not significant. Scale bars: 50 µm (B) and 100 µm (C).

mechanisms utilized by glioma cells *in vivo* in the brain, still requires further investigation.

Because of their prominent mechanotransducing functions to multiple ligands, integrins have been considered for therapeutic intervention to combat glioma cell dissemination in the brain tissue. Targeting αVβ3 and αVβ5 integrins using an RGD-mimicking cyclic peptide, cilengitide (Dechantsreiter et al., 1999), demonstrated promising pre-clinical efficacy in reducing glioma invasion in mouse and rat brains (Ishida et al., 2014; Onishi et al., 2013). However, recent phase II and III clinical trials in late-stage

Journal of Cell Science (2018) 131, jcs216382. doi:10.1242/jcs.216382

glioblastoma patients did not show efficacy of cilengitide in improving overall survival (Khasraw et al., 2016; Mason, 2015; Nabors et al., 2015; Stupp et al., 2014). Thus, mono-targeted interference with αVβ3 and αVβ5 integrins may not suffice to halt or revert glioma progression. The inefficiency of cilengitide to improve outcome is in line with the comparably weak effects we observed for αV integrin targeting in reducing glioma migration on basement membrane-related substrates, since cilengitide does not interfere with the adhesion functions of laminin and collagen IV binding integrins (α1β1, α2β1, α3β1, α6β1, α7β1 and α6β4). Preclinical antibody-based targeting of α7 or β1 integrin subunits results in a significant reduction in invasion of implanted glioma cells in the mouse brain but with a notable (up to 40–50%) residual invasion distance (Carbonell et al., 2013; Haas et al., 2017). Obviously, combined anti-αV and -β1 integrin targeting to interfere with preclinical and clinical glioma progression warrants further investigation. In line with available preclinical and clinical data, our findings indicate that overlapping integrin-dependent and, possibly, integrin-independent adhesion systems support glioma cell invasion and dissemination in brain tissue, as also observed in other cell models and tumour types (Balzer et al., 2012; Bergert et al., 2015; Hegerfeldt et al., 2002). The resilience of glioma cell migration in complex environments despite stringent molecular interference raises the concern that even multi-targeted anti-integrin adhesion perturbation may at best delay but not abrogate invasive progression of gliomas *in vivo* and thus will require additional combinatorial strategies designed to prevent adhesion plasticity and switching of invasion routes in brain tissue.

MATERIALS AND METHODS

Antibodies and reagents

Antibodies used for flow cytometry, immunofluorescence staining and for integrin targeting are listed in Table S1. Isotype-matched non-specific mouse or rat IgGs were used for antibody staining (FACS, IF) for background controls, or in integrin-targeting experiments as control non-adhesion perturbing antibodies. cRGDfV (cyclo Arg-Gly-Asp-D-Phe-Val; BACHEM, H-2574) and control cRADfV (cyclo Arg-Ala-Asp-D-Phe-Val; BACHEM, H-4088) peptides were used in migration assays to interfere with αVβ3, αVβ5 and α5β1 integrins (Belvisi et al., 2006; Pfaff et al., 1994; Shono et al., 2001; Zimmermann et al., 2005). cRGDfV peptide inhibits the following ligand interactions with purified integrins: fibrinogen-αIIbβ3, vitronectin-αVβ3, fibronectin-α5β1, echistatin-αVβ3 and -αVβ5, with IC50 varying from 2.5 nM to 6.4 µM (Belvisi et al., 2006; Dechantsreiter et al., 1999; Pfaff et al., 1994). To maximize inhibition, 50 µM cRGDfV peptide was used for function-blocking studies, in line with reported doses required to abrogate binding of αVβ3integrin with fibronectin (50 µM) or vitronectin (50 nM) (Shono et al., 2001). Growth factor-reduced rBM (Matrigel; Corning, Cat: 356231) was used as an undiluted solution in migration assays (≈9.8 mg/ml) or after dilution for coating culture plastic (30 µg/ml in PBS). Recombinant human laminin 511, laminin 211 (both from BioLamina), human placenta-derived type IV collagen (Advanced Bio Matrix) and fibronectin from human blood plasma (Sigma) were used for coating culture plastic (10 µg/ml in PBS).

Cell lines and culture

Human glioblastoma U-251MG cells (kind gift from Dr Joost Schalkwijk, Dept. of Dermatology, Radboudumc, Nijmegen, The Netherlands) and E-98 cells (Claes et al., 2008; Navis et al., 2015) were propagated *in vitro* in flasks for up to passage 35. The identity of tumour cells was verified by short tandem repeat (STR) DNA profiling (IDEXX BioResearch). No mammalian interspecies contamination was detected. STR of E-98 cells was generated for the first time, as follows: AMEL, X,Y; CSF1PO, 7,10; D13S317, 11; D16S539, 11; D5S818, 11,12; D7S820, 9,11; TH01, 8,9.3; TPOX, 8; vWA, 16,17. This profile does not match any other reported profile in the DSMZ STR database (Leibniz Institute DSMZ, German Collection of Microorganisms and Cell Cultures GmbH). Cells were routinely tested for mycoplasma contamination (Myco Alert, Lonza). Histone2B-eGFP (H2B/eGFP)-expressing U-251 and E-98 cells were generated by lentiviral transduction with pLenti6.2/V5-DEST Gateway (Invitrogen) containing H2B-eGFP. Primary mouse astrocytes immortalized with SV40 large T antigen and additionally transformed with retrovirus pBabe puro H-Ras V12 (Depner et al., 2016; Sawamiphak et al., 2010) were kindly provided by Dr Amparo Acker-Palmer, Frankfurt, Germany. Primary human astrocytes immortalized with SV40 large T antigen, were used as a reference.

Glioma cells and astrocytes were cultured in complete Dulbecco's Modified Eagle's Medium (DMEM; Invitrogen) supplemented with 10% fetal bovine serum (Sigma-Aldrich), penicillin (100 U/ml) and streptomycin (100 µg/ml; both PAA), L-glutamine (2 mM, Invitrogen) and sodium pyruvate (1 mM; Invitrogen).

Generation of glioma cell spheroids

U-251 and E-98 cell spheroids were generated using the hanging drop method, as described (Gritsenko et al., 2017). In brief, cells were detached from subconfluent culture (1 mM EDTA, 0.075% trypsin), washed, and maintained for 24 h in complete DMEM with methylcellulose (2.4%; Sigma) as hanging droplets (25 µl) containing 1000 (U-251) or 2000 cells (E-98).

Interference with integrin expression and function

Integrin function was perturbed by subunit-specific mouse-anti-human monoclonal antibodies targeting β1 (4B4; 15 µg/ml), α6 (GOH3; 10 µg/ml) and αV (17E6; 10 µg/ml). Cyclic peptide cRGDfV targeting RGD-binding αVβ3, αVβ5 and α5β1 integrins was used at 50 µM to ensure efficient inhibition of integrin binding to various matrix molecules (Pfaff et al., 1994; Shono et al., 2001; Zimmermann et al., 2005). As negative controls, isotypic IgG (10-15 µg/ml) or not-functional cRADfV peptide (50 µM) were used. Antibodies and peptides were added to the culture medium 3 h after seeding to secure initial spheroid engagement with the substrate. To increase the stringency of multi-targeting, interfering antibodies and peptide were combined with transient down-regulation of β1 integrin expression by siRNA. Glioma cells were incubated with β1-integrin-targeted or non-targeting smart-pool siRNA (Dharmacon; 50 nM) in the presence of Lipofectamine-2000 (1:1000, Dharmacon) for 20 h, washed with growth medium, cultured for 4 h, aggregated for glioma cell spheroid generation (24 h, hanging drop assay) and monitored in migration assays for an additional 24-48 h. Efficiency of β1 integrin downregulation was assessed by flow cytometry of single cells after detachment with EDTA (2 mM) 2-4 days after transfection.

Reconstituted basement membrane migration assays

Glioma cell spheroids were placed on 96-well plates coated with growth factor-reduced rBM (30 µg/ml, 16-18 h, +4°C) and overlaid with medium. 3D rBM-hyaluronan interface cultures were generated by polymerizing rBM on a culture dish (30 min, 37°C), followed by addition of glioma spheroids (2 h, 37°C) and complete DMEM supplemented with hyaluronan (10 mg/ml; Sigma), as described (Gritsenko et al., 2017). Migration efficacy was analysed after 24 h culture in fixed samples (4% PFA) using bright-field or confocal microscopy.

Invasion into murine brain slices

Glioma cell invasion from multicellular spheroids was probed using 3D murine brain slice culture, as described (Gritsenko et al., 2017). In brief, brains were dissected from 5- to 6-week-old female mice (Charles River or Jackson Laboratories) C57BL/6-Tg(TcraTcrb)1100Mjb/Crl (OT1), which were crossed with B6.Cg-Tg(CAG-DsRed*MST)1Nagy/J (dsRed) in our laboratory to introduce red fluorescent brain stroma. 400-µm-thick tissue slices were freshly sectioned using a vibratome (Leica, VT100s) and maintained on transwell insert membranes (Costar, 12-well plate; 8 µm pore diameter) in complete DMEM (37°C, 5% CO_2) for 1 h. Glioma cell spheroids expressing H2B-eGFP were added (8-10 spheroids per slice), allowed to initially adhere to the substrate (3 h), and antibodies and peptides were then added. During culture, medium and inhibitors were refreshed after 24 h and migration efficacy was assessed after 48 h. Brain slices were fixed [4% paraformaldehyde (PFA), 1 h, room temperature], washed and stained

with human-specific anti-vimentin antibody to discriminate glioma cells from DsRed-expressing blood vessels.

3D astrocyte scaffold invasion assay

3D-astrocyte-derived scaffolds were generated by immortalized murine astrocytes maintained at high cell density in 96-well plates (20,000 cells/well, coated with growth-factor-reduced rBM) for 2 days resulting in consolidated scaffolds of up to three cell layers in thickness (~50 µm), as described (Gritsenko et al., 2017). Glioma cell spheroids expressing H2B-eGFP were cultured on top of astrocyte scaffolds for 2 days, fixed (30 min, 4% PFA) and stained to visualize glioma cells and astrocytes. Primary antibodies were visualized with secondary Alexa Fluor-conjugated goat anti-mouse or goat anti-rabbit polyclonal antibodies (Invitrogen; 5 µg/ml). Cell nuclei were stained with 4′,6-diamidino-2-phenylindole (DAPI; 2.5 µg/ml).

Microscopy and quantification of glioma cell migration

Confocal microscopy (Olympus FV1000) was performed using long working distance 20× NA 0.50 and 40× NA 0.80 objectives at a step size of 2-3 µm. Imaris v.6.1.5 software (Bitplane) was used for 3D reconstruction of *Z*-stacks. Widefield microscopy of glioma cell invasion was performed by automated high-content epifluorescence microscopy followed by image stitching (Leica DMI6000B). For quantitative image analysis, operator-assisted image segmentation of bright-field or confocal 3D stacks was performed (Fiji software, V.1.49 g; Schindelin et al., 2012). The average cell migration distance representing radial migration of glioma cells from spheroids was calculated according to the following formula: average distance of cell migration=$\sqrt{}$(total cell area/π)−$\sqrt{}$(spheroid area/π).

The number of glioma cells that had migrated from spheroids on laminin 511-coated surfaces was quantified from bright field images and in brain slice or astrocyte scaffold culture was quantified by confocal and epifluorescence microscopy using H2B-eGFP-positive glioma cell nuclei. The average cell migration distance, which reflects the speed of cell movement, was used as the main parameter to identify cooperating integrin systems in glioma cell migration. Glioma cells associated with blood vessels in mouse brain slices were quantified as percentage of the total number of glioma cells invading from multicellular spheroids from 3D confocal stacks by manual image analysis.

Mass spectrometry

To identify proteins deposited during murine and human astrocyte culture on plastic dishes after 3 or 7 days, respectively, cells were detached (2 mM EDTA in PBS), remnants of cells solubilized (0.25% Triton X-100, 0.25% sodium deoxycholate in PBS), and adsorbed proteins were harvested by scraping (disposable cell scraper, Greiner bio-one). The resulting protein fraction was centrifuged (4250 ***g***, 45 min), the sediment dissolved (8 M urea, 3% SDS, 5% β-mercaptoethanol), separated electrophoretically on a 12% gel (TGX, Bio-Rad) for 30 min and digested with trypsin.

After extraction from the gel, the digested sample was loaded on a STAGE-tip (Stop And Go Elution, C18-reversed phase SPE) for desalting and concentration. Peptides were separated on a nanoLC system using a reversed phase C18 column coupled to a LTQ FT Ultra mass spectrometer (Thermo Fisher Scientific; Radboud Proteomics Centre, Radboudumc, Nijmegen). Peptide analysis was performed using a customized database consisting of the RefSeq protein database with *Mus musculus* or *Homo sapiens*, together with *Bos taurus* taxonomies to identify possible contaminating proteins originating from fetal bovine serum used for cell culture. Validation of peptide and protein identifications was carried out by applying score thresholds to minimize false-positive identification of emPAI values and number of peptides identified per protein. emPAI values were calculated as: emPAI=$[10^{(N\text{observed}/N\text{observable})}]-1$, where N_{observed} is the number of experimentally observed peptides and $N_{\text{observable}}$ is the calculated number of observable peptides for each protein (Ishihama et al., 2005).

Acknowledgements

We are thankful to Prof. Amparo Acker-Palmer for immortalized mouse astrocytes and William Leenders and Michael Weiger for constructive comments on the manuscript.

Competing interests

The authors declare no competing or financial interests.

Author contributions

Conceptualization: P.G.G., P.F.; Methodology: P.G.G., P.F.; Investigation: P.G.G., P.F.; Writing - original draft: P.G.G., P.F.; Writing - review & editing: P.G.G., P.F.; Supervision: P.F.; Project administration: P.F.; Funding acquisition: P.F.

Funding

This work was supported by The Netherlands Organisation for Scientific Research (NWO-VICI 918.11.626), Pieken in the Delta Oost Nederland, the European Research Council (ERC-CoG Deepinsight, 617430), National Institutes of Health (U54 CA210184-01) and the Cancer Genomics Center, The Netherlands. Deposited in PMC for release after 12 months.

Supplementary information

Supplementary information available online at
http://jcs.biologists.org/lookup/doi/10.1242/jcs.216382.supplemental

References

Ananthanarayanan, B., Kim, Y. and Kumar, S. (2011). Elucidating the mechanobiology of malignant brain tumors using a brain matrix-mimetic hyaluronic acid hydrogel platform. *Biomaterials* **32**, 7913-7923.

Balzer, E. M., Tong, Z., Paul, C. D., Hung, W.-C., Stroka, K. M., Boggs, A. E., Martin, S. S. and Konstantopoulos, K. (2012). Physical confinement alters tumor cell adhesion and migration phenotypes. *FASEB J. Off. Publ. Fed. Am. Soc. Exp. Biol.* **26**, 4045-4056.

Beadle, C., Assanah, M. C., Monzo, P., Vallee, R., Rosenfeld, S. S. and Canoll, P. (2008). The role of myosin II in glioma invasion of the brain. *Mol. Biol. Cell* **19**, 3357-3368.

Bello, L., Francolini, M., Marthyn, P., Zhang, J., Carroll, R. S., Nikas, D. C., Strasser, J. F., Villani, R., Cheresh, D. A. and Black, P. M. (2001). avb3 and avb5 Integrin Expression in Glioma Periphery. *Neurosurgery* **49**, 380-390.

Belvisi, L., Bernardi, A., Colombo, M., Manzoni, L., Potenza, D., Scolastico, C., Giannini, G., Marcellini, M., Riccioni, T., Castorina, M. et al. (2006). Targeting integrins: insights into structure and activity of cyclic RGD pentapeptide mimics containing azabicycloalkane amino acids. *Bioorg. Med. Chem.* **14**, 169-180.

Benton, G., Arnaoutova, I., George, J., Kleinman, H. K. and Koblinski, J. (2014). Matrigel: from discovery and ECM mimicry to assays and models for cancer research. *Adv. Drug Deliv. Rev.* **79-80**, 3-18.

Bergert, M., Erzberger, A., Desai, R. A., Aspalter, I. M., Oates, A. C., Charras, G., Salbreux, G. and Paluch, E. K. (2015). Force transmission during adhesion-independent migration. *Nat. Cell Biol.* **17**, 524-529.

Bjerkvig, R. (1986). Reaggregation of fetal rat brain cells in a stationary culture system. II: Ultrastructural characterization. *In Vitro Cell. Dev. Biol.* **22**, 193-200.

de Bouard, S., Christov, C., Guillamo, J.-S., Kassar-Duchossoy, L., Palfi, S., Leguerinel, C., Masset, M., Cohen-Hagenauer, O., Peschanski, M. and Lefrancois, T. (2002). Invasion of human glioma biopsy specimens in cultures of rodent brain slices: a quantitative analysis. *J. Neurosurg.* **97**, 169-176.

Carbonell, W. S., Delay, M., Jahangiri, A., Park, C. C. and Aghi, M. K. (2013). Beta1 Integrin targeting potentiates antiangiogenic therapy and inhibits the growth of bevacizumab-resistant glioblastoma. *Cancer Res.* **73**, 3145-3154.

Claes, A., Schuuring, J., Boots-Sprenger, S., Hendriks-Cornelissen, S., Dekkers, M., van der Kogel, A. J., Leenders, W. P., Wesseling, P. and Jeuken, J. W. (2008). Phenotypic and genotypic characterization of orthotopic human glioma models and its relevance for the study of anti-glioma therapy. *Brain Pathol.* **18**, 423-433.

Cuddapah, V. A., Robel, S., Watkins, S. and Sontheimer, H. (2014). A neurocentric perspective on glioma invasion. *Nat. Rev. Neurosci.* **15**, 455-465.

Dechantsreiter, M. A., Planker, E., Mathä, B., Lohof, E., Hölzemann, G., Jonczyk, A., Goodman, S. L. and Kessler, H. (1999). N-Methylated cyclic RGD peptides as highly active and selective alpha(V)beta(3) integrin antagonists. *J. Med. Chem.* **42**, 3033-3040.

Delamarre, E., Taboubi, S., Mathieu, S., Bérenguer, C., Rigot, V., Lissitzky, J., Figarella-branger, D. and Ouafik, L. H. (2009). Expression of integrin alpha6 beta1 enhances tumorigenesis in glioma cells. *Am J Pathol.* **175**, 844-855.

Demircioglu, F. and Hodivala-Dilke, K. (2016). alphavbeta3 integrin and tumour blood vessels-learning from the past to shape the future. *Curr. Opin. Cell Biol.* **42**, 121-127.

Depner, C., Zum Buttel, H., Böğürcü, N., Cuesta, A. M., Aburto, M. R., Seidel, S., Finkelmeier, F., Foss, F., Hofmann, J., Kaulich, K. et al. (2016). EphrinB2 repression through ZEB2 mediates tumour invasion and anti-angiogenic resistance. *Nat. Commun.* **7**, 12329.

Di Russo,, J., Hannocks, M.-J., Luik, A.-L., Song, J., Zhang, X., Yousif, L., Aspite, G., Hallmann, R. and Sorokin, L. (2017). Vascular laminins in physiology and pathology. *Matrix Biol.* **57–58**, 140-148.

Farin, A., Suzuki, S. O., Weiker, M., Goldman, J. E., Bruce, J. N. and Canoll, P. (2006). Transplanted glioma cells migrate and proliferate on host brain vasculature: a dynamic analysis. *Glia* **53**, 799-808.
Fayzullin, A., Tuvnes, F. A., Skjellegrind, H. K., Behnan, J., Mughal, A. A., Langmoen, I. A. and Vik-Mo, E. O. (2016). Time-lapse phenotyping of invasive glioma cells ex vivo reveals subtype-specific movement patterns guided by tumor core signaling. *Exp. Cell Res.* **349**, 199-213.
Frolov, A., Evans, I. M., Li, N., Sidlauskas, K., Paliashvili, K., Lockwood, N., Barrett, A., Brandner, S., Zachary, I. C. and Frankel, P. (2016). Imatinib and Nilotinib increase glioblastoma cell invasion via Abl-independent stimulation of p130Cas and FAK signalling. *Sci. Rep.* **6**, 27378.
Goodman, S. L. and Picard, M. (2012). Integrins as therapeutic targets. *Trends Pharmacol. Sci.* **33**, 405-412.
Gordon, V. D., Valentine, M. T., Gardel, M. L., Andor-Ardo, D., Dennison, S., Bogdanov, A. A., Weitz, D. A. and Deisboeck, T. S. (2003). Measuring the mechanical stress induced by an expanding multicellular tumor system: a case study. *Exp. Cell Res.* **289**, 58-66.
Gritsenko, P. G., Ilina, O. and Friedl, P. (2012). Interstitial guidance of cancer invasion. *J. Pathol.* **226**, 185-199.
Gritsenko, P., Leenders, W. and Friedl, P. (2017). Recapitulating in vivo-like plasticity of glioma cell invasion along blood vessels and in astrocyte-rich stroma. *Histochem. Cell Biol.* **148**, 395-406.
Haas, T. L., Sciuto, M. R., Brunetto, L., Valvo, C., Signore, M., Fiori, M. E., di Martino, S., Giannetti, S., Morgante, L., Boe, A. et al. (2017). Integrin alpha7 is a functional marker and potential therapeutic target in glioblastoma. *Cell Stem Cell* **21**, 35-50.e9.
Hamaia, S. W., Pugh, N., Raynal, N., Némoz, B., Stone, R., Gullberg, D., Bihan, D. and Farndale, R. W. (2012). Mapping of potent and specific binding motifs, GLOGEN and GVOGEA, for integrin alpha1beta1 using collagen toolkits II and III. *J. Biol. Chem.* **287**, 26019-26028.
Hegerfeldt, Y., Tusch, M., Brocker, E.-B. and Friedl, P. (2002). Collective cell movement in primary melanoma explants: plasticity of cell-cell interaction, beta1-integrin function, and migration strategies. *Cancer Res.* **62**, 2125-2130.
Hong, X., Sin, W. C., Harris, A. L. and Naus, C. C. (2015). Gap junctions modulate glioma invasion by direct transfer of microRNA. *Oncotarget* **6**, 15566-15577.
Hughes, C. S., Postovit, L. M. and Lajoie, G. A. (2010). Matrigel: a complex protein mixture required for optimal growth of cell culture. *Proteomics* **10**, 1886-1890.
Ido, H., Harada, K., Futaki, S., Hayashi, Y., Nishiuchi, R., Natsuka, Y., Li, S., Wada, Y., Combs, A. C., Ervasti, J. M. et al. (2004). Molecular dissection of the alpha-dystroglycan- and integrin-binding sites within the globular domain of human laminin-10. *J. Biol. Chem.* **279**, 10946-10954.
Ishida, J., Onishi, M., Kurozumi, K., Ichikawa, T., Fujii, K., Shimazu, Y., Oka, T. and Date, I. (2014). Integrin inhibitor suppresses bevacizumab-induced glioma invasion. *Transl. Oncol.* **7**, 292-302.e1.
Ishihama, Y., Oda, Y., Tabata, T., Sato, T., Nagasu, T., Rappsilber, J. and Mann, M. (2005). Exponentially modified protein abundance index (emPAI) for estimation of absolute protein amount in proteomics by the number of sequenced peptides per protein. *Mol. Cell. Proteomics* **4**, 1265-1272.
Katsetos, C. D., Reginato, M. J., Baas, P. W., D'Agostino, L., Legido, A., Tuszyn Ski, J. A., Dráberová, E. and Dráber, P. (2015). Emerging microtubule targets in glioma therapy. *Semin. Pediatr. Neurol.* **22**, 49-72.
Kaufman, L. J., Brangwynne, C. P., Kasza, K. E., Filippidi, E., Gordon, V. D., Deisboeck, T. S. and Weitz, D. A. (2005). Glioma expansion in collagen I matrices: analyzing collagen concentration-dependent growth and motility patterns. *Biophys. J.* **89**, 635-650.
Kawataki, T., Yamane, T., Naganuma, H., Rousselle, P., Andurén, I., Tryggvason, K. and Patarroyo, M. (2007). Laminin isoforms and their integrin receptors in glioma cell migration and invasiveness: evidence for a role of alpha5-laminin(s) and alpha3beta1 integrin. *Exp. Cell Res.* **313**, 3819-3831.
Khasraw, M., Lee, A., McCowatt, S., Kerestes, Z., Buyse, M. E., Back, M., Kichenadasse, G., Ackland, S. and Wheeler, H. (2016). Cilengitide with metronomic temozolomide, procarbazine, and standard radiotherapy in patients with glioblastoma and unmethylated MGMT gene promoter in ExCentric, an open-label phase II trial. *J. Neurooncol.* **128**, 163-171.
Khoshnoodi, J., Pedchenko, V. and Hudson, B. G. (2008). Mammalian collagen IV. *Microsc. Res. Tech.* **71**, 357-370.
Kikkawa, Y., Sasaki, T., Nguyen, M. T., Nomizu, M., Mitaka, T. and Miner, J. H. (2007). The LG1-3 tandem of laminin alpha5 harbors the binding sites of Lutheran/basal cell adhesion molecule and alpha3beta1/alpha6beta1 integrins. *J. Biol. Chem.* **282**, 14853-14860.
Kikkawa, Y., Ogawa, T., Sudo, R., Yamada, Y., Katagiri, F., Hozumi, K., Nomizu, M. and Miner, J. H. (2013). The lutheran/basal cell adhesion molecule promotes tumor cell migration by modulating integrin-mediated cell attachment to laminin-511 protein. *J. Biol. Chem.* **288**, 30990-31001.
Lin, L. and Kurpakus-Wheater, M. (2002). Laminin alpha5 chain adhesion and signaling in conjunctival epithelial cells. *Invest. Ophthalmol. Vis. Sci.* **43**, 2615-2621.
Mason, W. P. (2015). End of the road: confounding results of the CORE trial terminate the arduous journey of cilengitide for glioblastoma. *Neuro. Oncol.* **17**, 634-635.
Miyata, S. and Kitagawa, H. (2017). Formation and remodeling of the brain extracellular matrix in neural plasticity: roles of chondroitin sulfate and hyaluronan. *Biochim. Biophys. Acta* **1861**, 2420-2434.
Nabors, L. B., Fink, K. L., Mikkelsen, T., Grujicic, D., Tarnawski, R., Nam, D. H., Mazurkiewicz, M., Salacz, M., Ashby, L., Zagonel, V. et al. (2015). Two cilengitide regimens in combination with standard treatment for patients with newly diagnosed glioblastoma and unmethylated MGMT gene promoter: results of the open-label, controlled, randomized phase II CORE study. *Neuro. Oncol.* **17**, 708-717.
Nakada, M., Nambu, E., Furuyama, N., Yoshida, Y., Takino, T., Hayashi, Y., Sato, H., Sai, Y., Tsuji, T., Miyamoto, K. et al. (2013). Integrin α3 is overexpressed in glioma stem-like cells and promotes invasion. *Br. J. Cancer* **108**, 2516-2524.
Navis, A. C., van Lith, S. A. M., van Duijnhoven, S. M. J., de Pooter, M., Yetkin-Arik, B., Wesseling, P., Hendriks, W. J. A. J., Venselaar, H., Timmer, M., van Cleef, P. et al. (2015). Identification of a novel MET mutation in high-grade glioma resulting in an auto-active intracellular protein. *Acta Neuropathol.* **130**, 131-144.
Nielsen, P. K. and Yamada, Y. (2001). Identification of cell-binding sites on the Laminin alpha 5 N-terminal domain by site-directed mutagenesis. *J. Biol. Chem.* **276**, 10906-10912.
Nishiuchi, R., Murayama, O., Fujiwara, H., Gu, J., Kawakami, T., Aimoto, S., Wada, Y. and Sekiguchi, K. (2003). Characterization of the ligand-binding specificities of integrin alpha3beta1 and alpha6beta1 using a panel of purified laminin isoforms containing distinct alpha chains. *J. Biochem.* **134**, 497-504.
Nishiuchi, R., Takagi, J., Hayashi, M., Ido, H., Yagi, Y., Sanzen, N., Tsuji, T., Yamada, M. and Sekiguchi, K. (2006). Ligand-binding specificities of laminin-binding integrins: a comprehensive survey of laminin-integrin interactions using recombinant alpha3beta1, alpha6beta1, alpha7beta1 and alpha6beta4 integrins. *Matrix Biol.* **25**, 189-197.
Oliveira, R., Christov, C., Guillamo, J. S., de Boüard, S., Palfi, S., Venance, L., Tardy, M. and Peschanski, M. (2005). Contribution of gap junctional communication between tumor cells and astroglia to the invasion of the brain parenchyma by human glioblastomas. *BMC Cell Biol.* **6**, 7.
Onishi, M., Ichikawa, T., Kurozumi, K., Fujii, K., Yoshida, K., Inoue, S., Michiue, H., Chiocca, E. A., Kaur, B. and Date, I. (2013). Bimodal anti-glioma mechanisms of cilengitide demonstrated by novel invasive glioma models. *Neuropathology* **33**, 162-174.
Panopoulos, A., Howell, M., Fotedar, R. and Margolis, R. L. (2011). Glioblastoma motility occurs in the absence of actin polymer. *Mol. Biol. Cell* **22**, 2212-2220.
Paul, C. D., Mistriotis, P. and Konstantopoulos, K. (2017). Cancer cell motility: lessons from migration in confined spaces. *Nat. Rev. Cancer* **17**, 131-140.
Paulus, W., Baur, I., Schuppan, D. and Roggendorf, W. (1993). Characterization of integrin receptors in normal and neoplastic human brain. *Am. J. Pathol.* **143**, 154-163.
Pedchenko, V., Zent, R. and Hudson, B. G. (2004). Alpha(v)beta3 and alpha(v)beta5 integrins bind both the proximal RGD site and non-RGD motifs within noncollagenous (NC1) domain of the alpha3 chain of type IV collagen: implication for the mechanism of endothelia cell adhesion. *J. Biol. Chem.* **279**, 2772-2780.
Pfaff, M., Tangemann, K., Muller, B., Gurrath, M., Muller, G., Kessler, H., Timpl, R. and Engel, J. (1994). Selective recognition of cyclic RGD peptides of NMR defined conformation by alpha IIb beta 3, alpha V beta 3, and alpha 5 beta 1 integrins. *J. Biol. Chem.* **269**, 20233-20238.
Pouliot, N. and Kusuma, N. (2013). Laminin-511 A multi-functional adhesion protein regulating cell migration, tumor invasion and metastasis. *Cell Adh. Migr.* **7**, 142-149.
Ramovs, V., Te Molder, L. and Sonnenberg, A. (2017). The opposing roles of laminin-binding integrins in cancer. *Matrix Biol.* **57–58**, 213-243.
Rao, S. S., Lannutti, J. J., Viapiano, M. S., Sarkar, A. and Winter, J. O. (2014). Toward 3D biomimetic models to understand the behavior of glioblastoma multiforme cells. *Tissue Eng. Part B. Rev.* **20**, 314-327.
Rape, A., Ananthanarayanan, B. and Kumar, S. (2014). Engineering strategies to mimic the glioblastoma microenvironment. *Adv. Drug Deliv. Rev.* **79–80**, 172-183.
Rath, B. H., Fair, J. M., Jamal, M., Camphausen, K. and Tofilon, P. J. (2013). Astrocytes enhance the invasion potential of glioblastoma stem-like cells. *PLoS One* **8**, e54752.
Sasaki, T. and Timpl, R. (2001). Domain IVa of laminin alpha5 chain is cell-adhesive and binds beta1 and alphaVbeta3 integrins through Arg-Gly-Asp. *FEBS Lett.* **509**, 181-185.
Sawamiphak, S., Seidel, S., Essmann, C. L., Wilkinson, G. A., Pitulescu, M. E., Acker, T. and Acker-Palmer, A. (2010). Ephrin-B2 regulates VEGFR2 function in developmental and tumour angiogenesis. *Nature* **465**, 487-491.
Schaller, M. D. (2001). Paxillin: a focal adhesion-associated adaptor protein. *Oncogene* **20**, 6459-6472.
Schindelin, J., Arganda-Carreras, I., Frise, E., Kaynig, V., Longair, M., Pietzsch, T., Preibisch, S., Rueden, C., Saalfeld, S., Schmid, B. et al. (2012). Fiji: an open-source platform for biological-image analysis. *Nat. Methods* **9**, 676-682.
Schittenhelm, J., Schwab, E. I., Sperveslage, J., Tatagiba, M., Meyermann, R., Fend, F., Goodman, S. L. and Sipos, B. (2013). Longitudinal expression analysis of αv integrins in human gliomas reveals upregulation of integrin αvβ3 as a negative prognostic factor. *J. Neuropathol. Exp. Neurol.* **72**, 194-210.

Shimizu, H., Hosokawa, H., Ninomiya, H., Miner, J. H. and Masaki, T. (1999). Adhesion of cultured bovine aortic endothelial cells to laminin-1 mediated by dystroglycan. *J. Biol. Chem.* **274**, 11995-12000.

Shono, T., Mochizuki, Y., Kanetake, H. and Kanda, S. (2001). Inhibition of FGF-2-mediated chemotaxis of murine brain capillary endothelial cells by cyclic RGDfV peptide through blocking the redistribution of c-Src into focal adhesions. *Exp. Cell Res.* **268**, 169-178.

Sonnenberg, A., Janssen, H., Hogervorst, F., Calafat, J. and Hilgers, J. (1987). A complex of platelet glycoproteins Ic and IIa identified by a rat monoclonal antibody. *J. Biol. Chem.* **262**, 10376-10383.

Spenlé, C., Simon-assmann, P., Orend, G. and Miner, J. H. (2013). Laminin α5 guides tissue patterning and organogenesis. *Cell Adh. Migr.* **7**, 90-100.

Stupp, R., Hegi, M. E., Gorlia, T., Erridge, S. C., Perry, J., Hong, Y.-K., Aldape, K. D., Lhermitte, B., Pietsch, T., Grujicic, D. et al. (2014). Cilengitide combined with standard treatment for patients with newly diagnosed glioblastoma with methylated MGMT promoter (CENTRIC EORTC 26071-22072 study): a multicentre, randomised, open-label, phase 3 trial. *Lancet. Oncol.* **15**, 1100-1108.

Thompson, E. G. and Sontheimer, H. (2016). A role for ion channels in perivascular glioma invasion. *Eur. Biophys. J.* **45**, 635-648.

Tonn, J. C., Wunderlich, S., Kerkau, S., Klein, C. E. and Roosen, K. (1998). Invasive behaviour of human gliomas is mediated by interindividually different integrin patterns. *Anticancer Res.* **18**, 2599-2605.

Vehlow, A., Klapproth, E., Storch, K., Dickreuter, E., Seifert, M., Dietrich, A., Butof, R., Temme, A. and Cordes, N. (2017). Adhesion- and stress-related adaptation of glioma radiochemoresistance is circumvented by beta1 integrin/JNK co-targeting. *Oncotarget* **8**, 49224-49237.

Watkins, S., Robel, S., Kimbrough, I. F., Robert, S. M., Ellis-Davies, G. and Sontheimer, H. (2014). Disruption of astrocyte-vascular coupling and the blood-brain barrier by invading glioma cells. *Nat. Commun.* **5**, 4196.

Wen, P. Y. and Reardon, D. A. (2016). Neuro-oncology in 2015: Progress in glioma diagnosis, classification and treatment. *Nat. Rev. Neurol.* **12**, 69-70.

Wondimu, Z., Omrani, S., Ishikawa, T., Javed, F., Oikawa, Y., Virtanen, I., Juronen, E., Ingerpuu, S. and Patarroyo, M. (2013). A novel monoclonal antibody to human laminin α5 chain strongly inhibits integrin-mediated cell adhesion and migration on laminins 511 and 521. *PLoS One* **8**, 14-24.

Wu, C., Ivars, F., Anderson, P., Hallmann, R., Vestweber, D., Nilsson, P., Robenek, H., Tryggvason, K., Song, J., Korpos, E. et al. (2009). Endothelial basement membrane laminin alpha5 selectively inhibits T lymphocyte extravasation into the brain. *Nat. Med.* **15**, 519-527.

Xu, J., Rodriguez, D., Petitclerc, E., Kim, J. J., Hangai, M., Moon, Y. S., Davis, G. E. and Brooks, P. C. (2001). Proteolytic exposure of a cryptic site within collagen type IV is required for angiogenesis and tumor growth in vivo. *J. Cell Biol.* **154**, 1069-1079.

Yousif, L. F., Di Russo,, J. and Sorokin, L. (2013). Laminin isoforms in endothelial and perivascular basement membranes. *Cell Adh. Migr.* **7**, 101-110.

Yurchenco, P. D. (2011). Basement membranes: cell scaffoldings and signaling platforms. *Cold Spring Harb. Perspect. Biol.* **3**, a004911.

Yurchenco, P. D. (2015). Integrating Activities of Laminins that Drive Basement Membrane Assembly and Function. *Curr. Top. Membr.* **76**, 1-30.

Zimmermann, D., Guthöhrlein, E. W., Malešević, M., Sewald, K., Wobbe, L., Heggemann, C. and Sewald, N. (2005). Integrin alpha5beta1 ligands: biological evaluation and conformational analysis. *Chembiochem* **6**, 272-276.

Supplementary Table 1. List of antibodies used for staining and perturbation of adhesion function of integrins.

Antigen	Species, clonality, labeling	Isotype	Clone name	Company	Catalogue number	Application	Final concentration µg/ml
Human α1 integrin	mouse monoclonal, FITC	IgG1	TS2/7	Abcam	ab34176	FACS	10
Human α2 integrin	mouse monoclonal, FITC	IgG1	AK-7	BD Biosciences	555498	FACS	5
Human α3 integrin	mouse monoclonal	IgG1	17C6	Bio-Rad	MCA1948 GA	FACS	10
Human α6 integrin	Rat monoclonal	IgG2a	GoH3	BD Biosciences	555734	FACS	10
Human αV integrin	mouse monoclonal	IgG1	272-17E6	Abcam	ab16821	FACS, Adhesion-perturbing	10
Human β1 integrin	mouse monoclonal	IgG1	4B4	Bechman Coulter	6603113	FACS, IF, Adhesion-perturbing	10 15
Human β3 integrin	mouse monoclonal	IgG1	Y2/51	Bio-Rad	MCA2588 GA	FACS	10
Human β4 integrin	mouse monoclonal	IgG1	ASC-3	Abcam	ab78267	FACS	10
Human Collagen IV	Rabbit polyclonal	IgG1	–	Sigma	PA1-28534	IF	5
Mouse laminin	Rabbit polyclonal	IgG	–	Sigma	L9393	IF	7
Human vimentin	Rabbit monoclonal	IgG	SP20	Thermo Scientific	MA5-14564	IF	1:250
Chicken paxillin	Mouse monoclonal	IgG1	165/ Paxillin	BD Biosciences	610619	IF	10
Isotype control	Mouse monoclonal	IgG1	MOPC-21	BD Biosciences	555746	FACS, IF, Adhesion-perturbing	10 10-15
Isotype control	Rat monoclonal	IgG2a	R35-95	BD Biosciences	553927	FACS, IF, Adhesion-perturbing	10
Isotype control, FITC	Mouse monoclonal	IgG1	MOPC-21	BD Biosciences	551955	FACS	10

Supplementary Table 2. Proteins deposited by mouse astrocytes on cell culture dish identified by mass-spectrometry. Details are described in Materials and Methods section.

Click here to Download Table S2

Supplementary Table 3. Proteins deposited by human astrocytes on cell culture dish identified by mass-spectrometry. Details are described in Materials and Methods section.

Click here to Download Table S3

Supplementary information

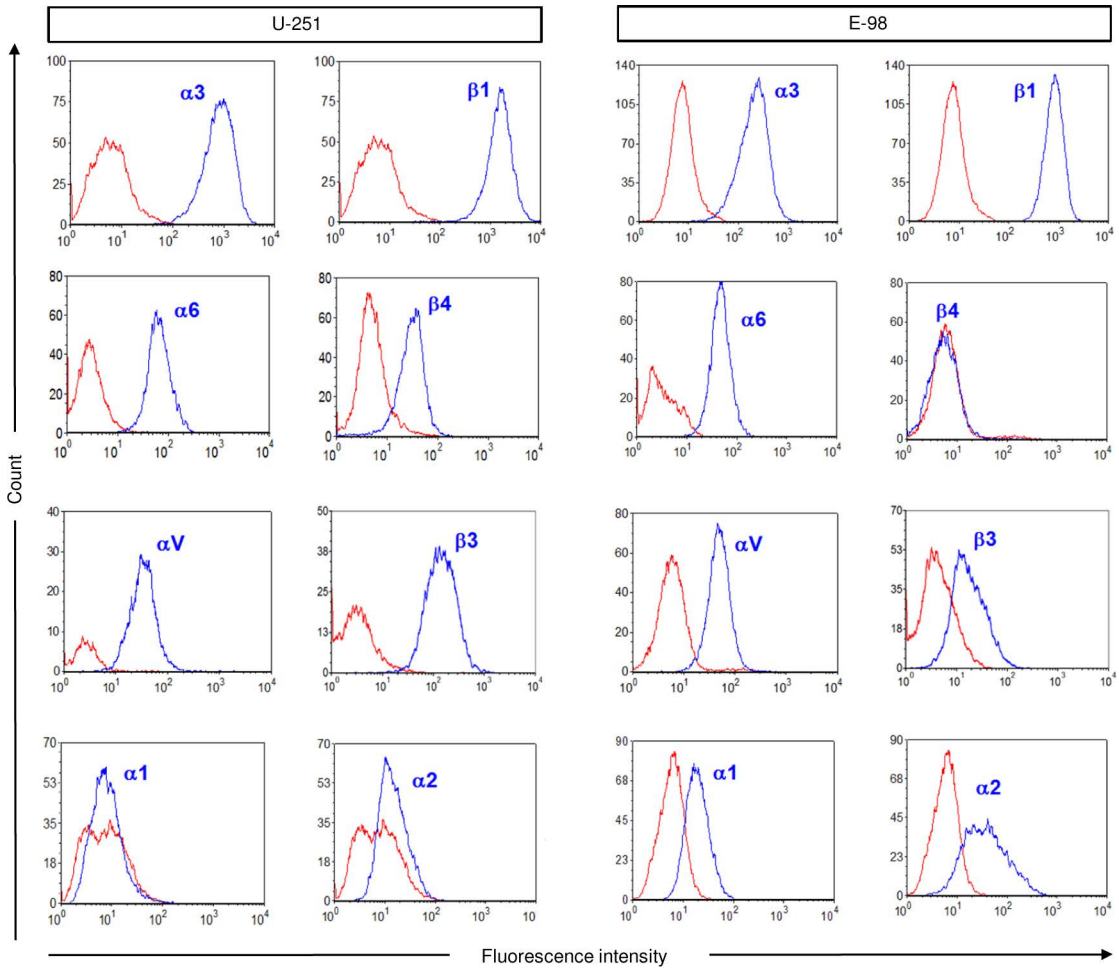

Fig. S1. Expression of integrin subunits in U-251 and E-98 cells measured with flow cytometry.

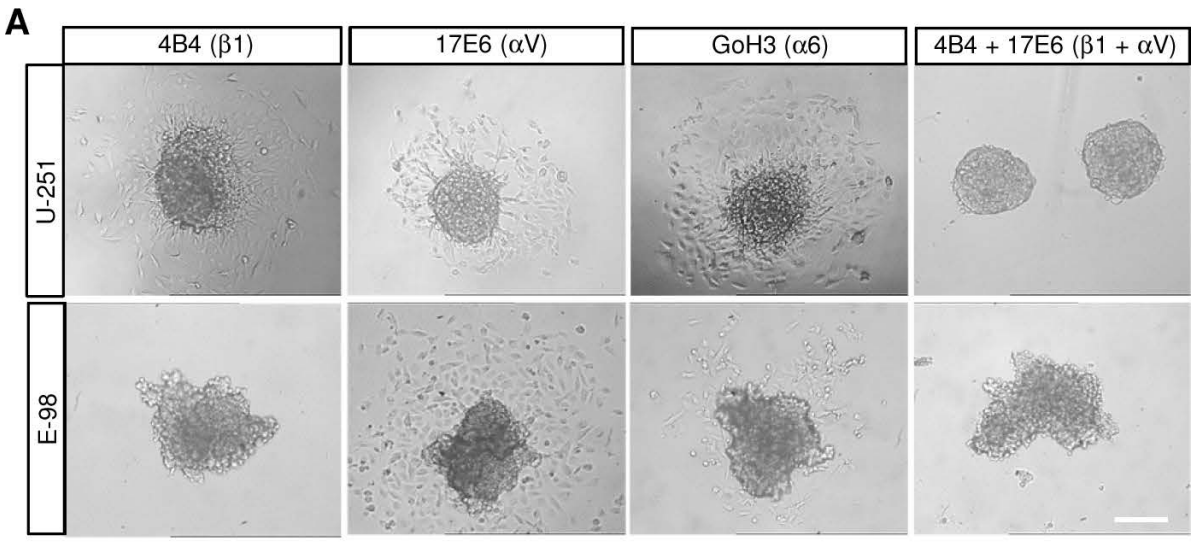

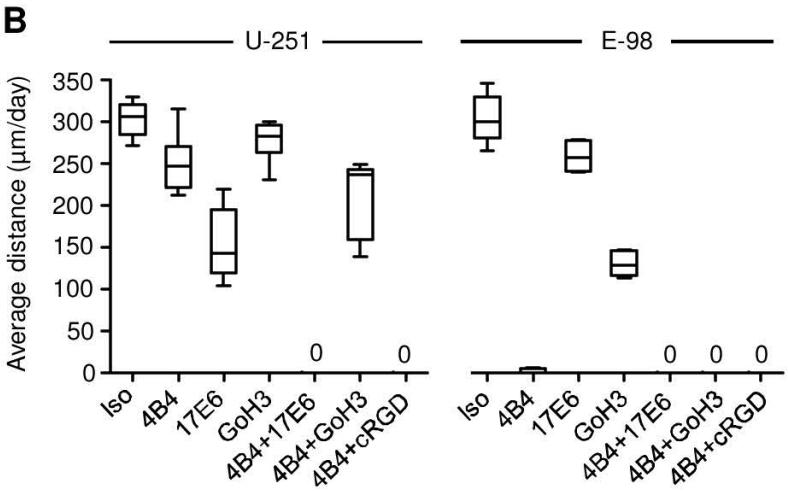

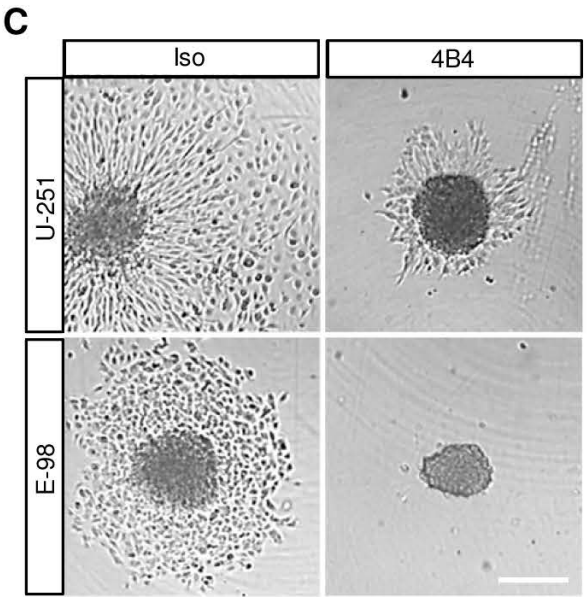

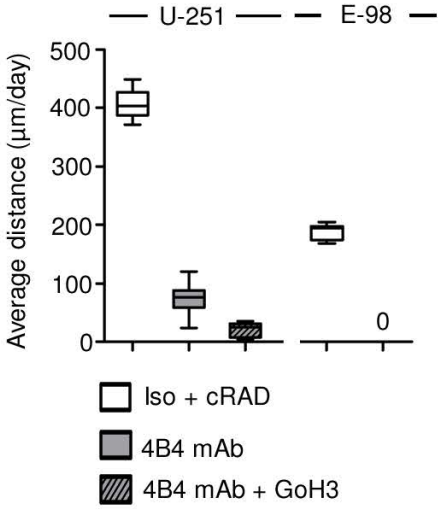

Fig. S2. Migration of glioma cells on rBM coated surface and in hyaluronan-rBM interface is dependent on β1, αV and α6 integrin subunits. (A) Radial migration of U-251 and E-98 cells from spheroids after 24 h on plastic surface coated with rBM molecules (Matrigel) in media with control isotype IgGs or with adhesion-perturbing anti-integrin mAbs 4B4 (β1), 17E6 (αV), GoH3 (α6) combined with cRGDfV peptide inhibiting RGD-binding integrins (α5, αV). (B) Average radial migration distance of U-251 and E-98 cells from the spheroid margin. Data represent 10-13 (U-251) and 10-11 (E-98) spheroids per condition from 2 independent experiments. Values display the median (black line), 25/75 percentiles (boxes) and maximum/minimum (whiskers). (C) Migration of U-251 and E-98 cells from spheroids along hyaluronan-rBM interface in media with control isotype IgGs or with adhesion-perturbing anti β1 integrin mAb 4B4 or anti α6 mAb GoH3. (D) Average migration distance of U-251 and E-98 cells along hyaluronan-rBM interface after 24 h. Data represent 10-14 (U-251) and 10-11 (E-98) spheroids per condition from 2 independent experiments. Values display the median (black line), 25/75 percentiles (boxes) and maximum/minimum (whiskers). Scale bars, 200 μm.

A

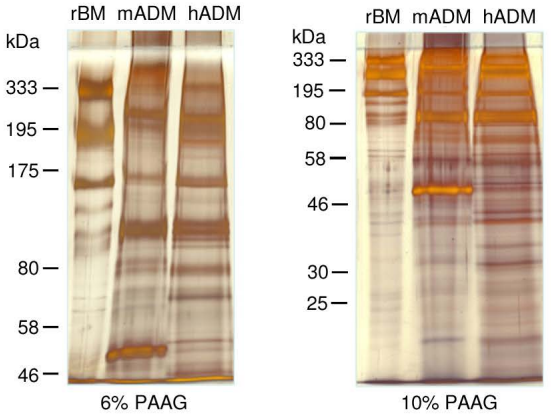

B

Matrix proteins identified both in mouse and human astrocyte matrices
nidogen-1
laminin subunit alpha-1
laminin subunit beta-1
laminin subunit gamma-1
perlecan
fibronectin
vitronectin *
collagen alpha-1(XVIII) *
laminin subunit alpha-5 *
* Proteins present in Matrigel in trace amounts

C

Proteins deposited by mouse astrocytes

PROTEIN	emPAI Sample 1	NR-PEPS Sample 1
serine protease HTRA1 precursor [Mus musculus]	2.26	17
tubulointerstitial nephritis antigen-like precursor [Mus musculus]	0.60	7
nidogen-1 precursor [Mus musculus]	0.54	16
cathelicidin-7 precursor [Bos taurus]	0.47	2
keratin 9 [Homo sapiens]	0.40	6
plasminogen activator inhibitor 1 precursor [Mus musculus]	0.39	6
vimentin [Mus musculus]	0.36	7
lysyl oxidase homolog 2 precursor [Mus musculus]	0.31	7
alpha-2-HS-glycoprotein precursor [Bos taurus]	0.28	3
keratin, type I cytoskeletal 14 [Bos taurus]	0.26	5
nidogen-1 precursor [Bos taurus]	0.25	10
PREDICTED: hemoglobin subunit beta-like [Bos taurus]	0.25	2
PREDICTED: keratin, type I cytoskeletal 10-like [Bos taurus]	0.23	4
actin, cytoplasmic 1 [Mus musculus]	0.21	3
keratin, type II cytoskeletal 1 [Mus musculus]	0.20	3
keratin, type I cytoskeletal 10 [Mus musculus]	0.17	3
laminin subunit beta-1 [Mus musculus]	0.17	9
vitronectin precursor [Bos taurus]	0.17	2
fibronectin precursor [Mus musculus]	0.16	11
keratin, type II cytoskeletal 6A [Bos taurus]	0.15	3
von Willebrand factor A domain-containing protein 1 precursor [Mus musculus]	0.15	2
PREDICTED: keratin, type II cytoskeletal 1 [Bos taurus]	0.14	3
laminin subunit gamma-1 precursor [Mus musculus]	0.13	7
PREDICTED: keratin, type I cytoskeletal 25-like [Bos taurus]	0.13	2
PREDICTED: keratin, type II cytoskeletal 2 epidermal [Bos taurus]	0.12	3
PREDICTED: keratin, type II cytoskeletal 3 [Bos taurus]	0.11	2
basement membrane-specific heparan sulfate proteoglycan core protein precursor [Mus musculus]	0.11	14
laminin subunit alpha-1 precursor [Mus musculus]	0.11	11
PREDICTED: keratin, type I cytoskeletal 13 [Bos taurus]	0.11	2
keratin, type II cytoskeletal 2 epidermal [Mus musculus]	0.10	3
collagen alpha-1(XVIII) chain isoform 2 precursor [Mus musculus]	0.10	4
lysyl oxidase homolog 4 isoform 1 precursor [Mus musculus]	0.10	3
keratin, type II cytoskeletal 7 [Bos taurus]	0.09	2
A disintegrin and metalloproteinase with thrombospondin motifs 1 precursor [Mus musculus]	0.06	2
prelamin-A/C isoform A [Mus musculus]	0.03	1
laminin subunit alpha-5 precursor [Mus musculus]	0.02	3

Fig. S3. Differences in protein composition of astrocyte-deposited matrix and rBM. (A) PAAG electrophoresis (in 6% and 10% gels) of rBM, mouse (mADM) and human (hADM) astrocyte deposited matrices (silver staining). (B) Matrix proteins identified both in mouse and human astrocyte matrix and low-abundance proteins in growth factor reduced rBM (Matrigel) based on published mass-spectrometry data (Hughes et al., 2010). (C) Proteins identified by mass-spectrometry in mouse astrocyte-deposited matrix.

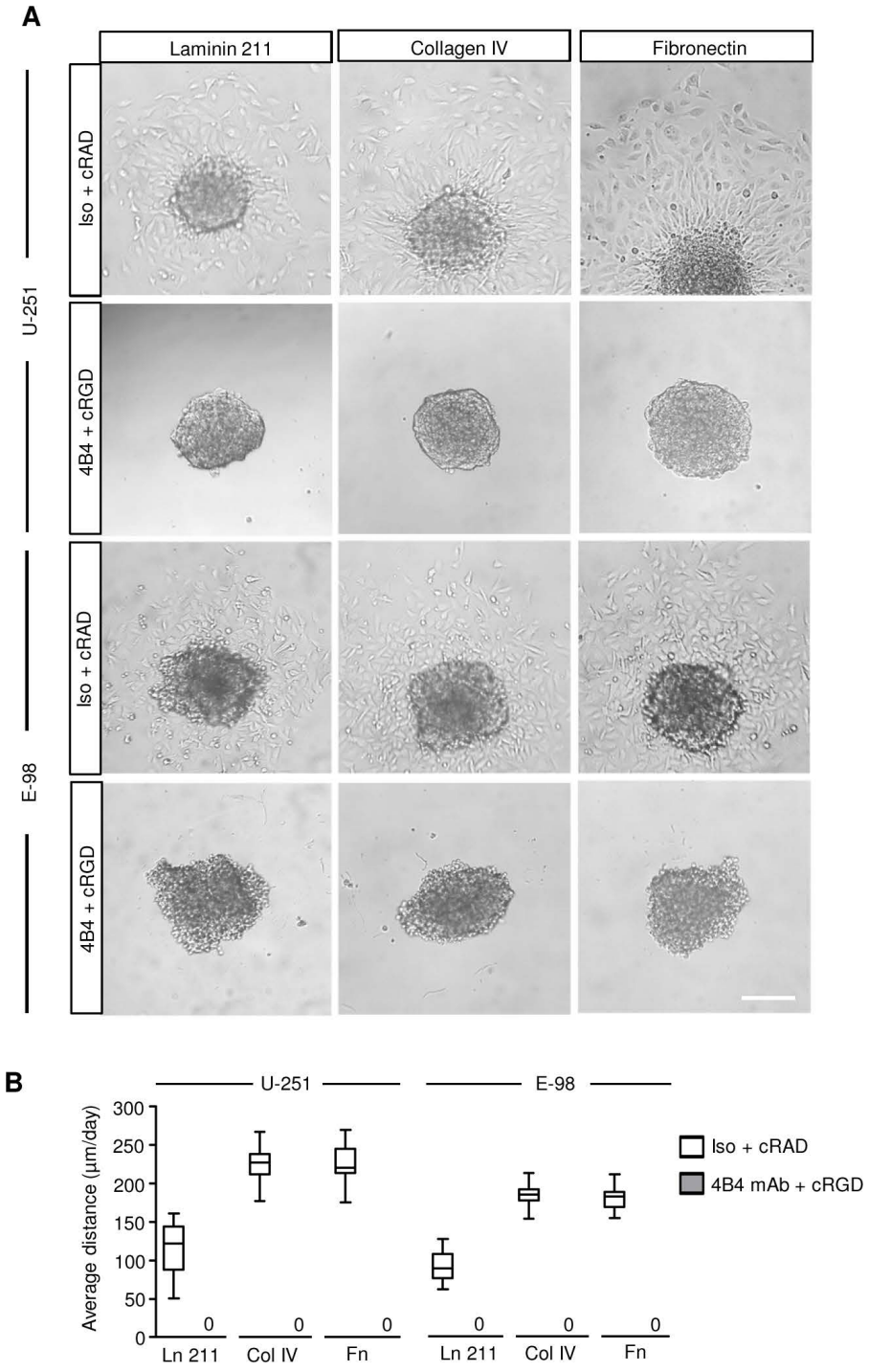

Fig. S4. Migration of glioma cells on laminin 211, collagen IV or fibronectin coated surface is dependent on β1 and αV integrin subunits. (A) Radial migration of U-251 and E-98 cells from spheroids after 24 h on plastic surface coated with the indicated matrix molecules. Isotypic IgG1 and control cRADfV peptide or adhesion-perturbing anti-β1 integrin 4B4 mAb combined with cRGDfV peptide inhibiting RGD-binding integrins (α5, αV) were added to the culture media. (B) Average migration distance of U-251 and E-98 cells on plastic surface coated with the indicated matrix molecules. Data represent 11-24 (U-251) and 16-25 (E-98) spheroids per condition from 2 independent experiments. Values display the median (black line), 25/75 percentiles (boxes) and maximum/minimum (whiskers). Scale bars, 200 µm.

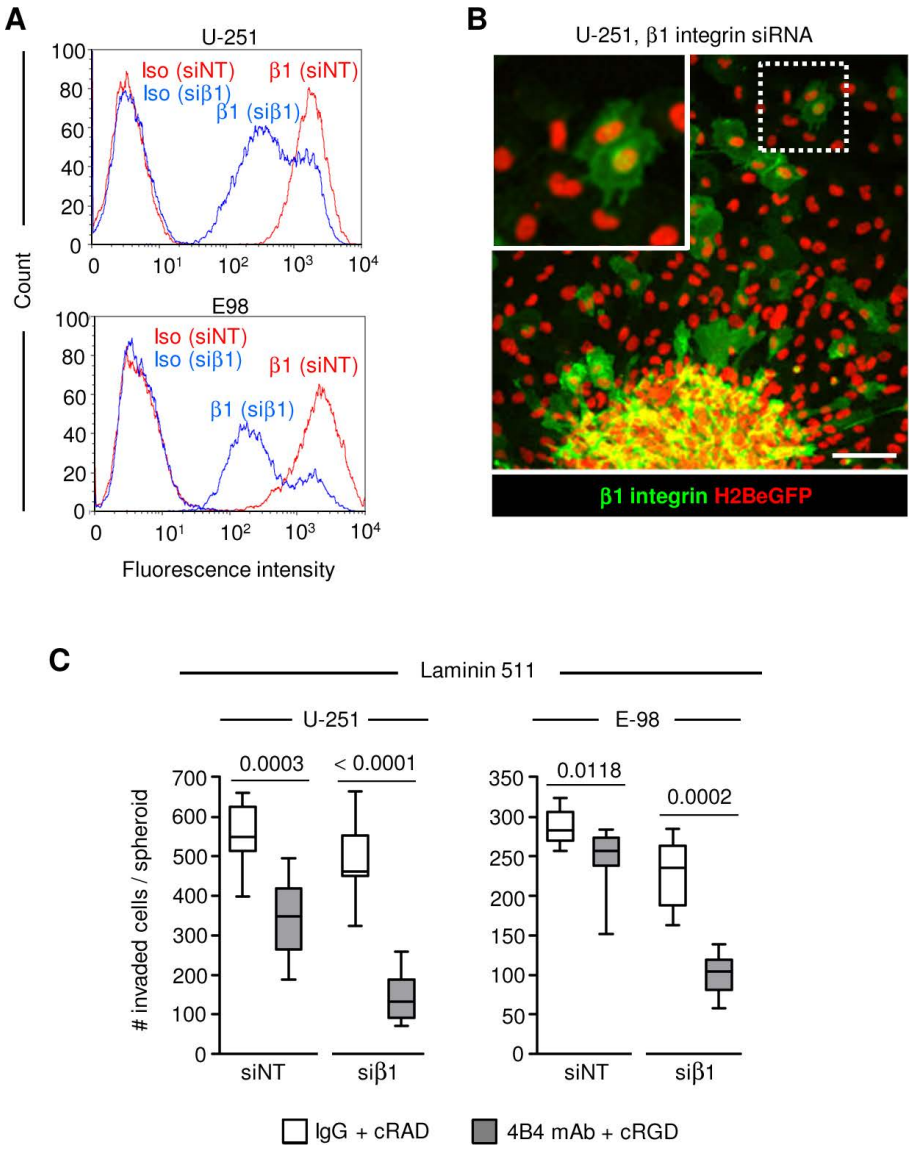

Fig. S5. β1 integrin subunits mediate glioma cell migration on laminin 511. Expression of β1 integrin in U-251 and E-98 cells 3 days after their transfection with either non-targeting (NT) or β1 integrin siRNA based on flow cytometry (A) or confocal microscopy on laminin 511 coated culture surface (B). Red nuclei, all cells; green fluorescence, cells retaining β1 integrin expression despite siRNA treatment. (C) Number of migrated U-251 and E-98 cells per spheroid after transfection with NT or anti-β1 integrin siRNAs from spheroids on laminin 511 coated culture surface (24 h), in media with isotypic IgG1 and control cRADfV peptide or adhesion-perturbing anti β1 integrin 4B4 mAb combined with cRGDfV peptide (related to Fig. 5B). Data represent 16-32 (U-251) and 15-24 (E-98) spheroids per condition from 3 independent siRNA transfections. Values display the median (black line), 25/75 percentiles (boxes) and maximum/minimum (whiskers). P-values shown were obtained using the Mann-Whitney test. Scale bar, 100 μm.

References.

Hughes, C. S., Postovit, L. M. and Lajoie, G. A. (2010). Matrigel : A complex protein mixture required for optimal growth of cell culture. *Proteomics* **10**, 1886–1890.